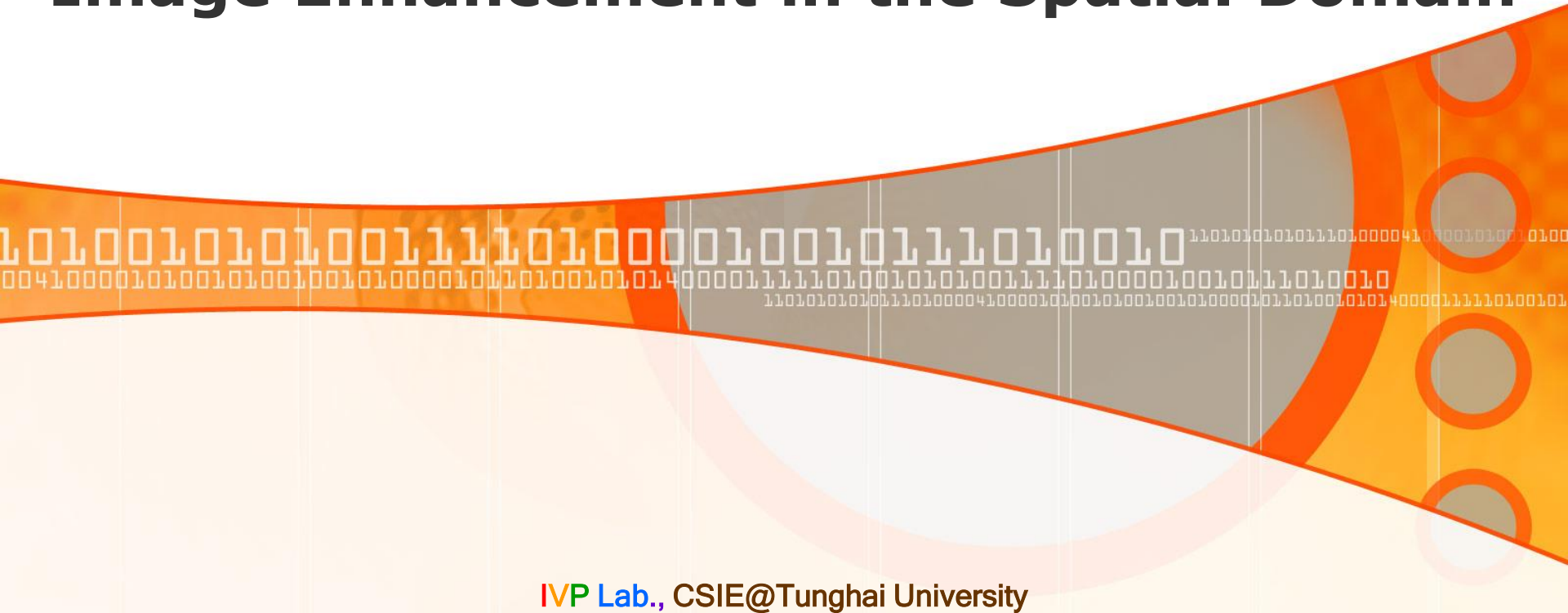


# Chapter 3

## Image Enhancement in the Spatial Domain



- *Spatial domain*
  - refers to the image plane itself, and approaches in this category are based on **direct manipulation of pixels** in an image
- *Frequency domain*
  - based on modifying the **Fourier transform** of an image

As indicated previously, the term *spatial domain* refers to the aggregate of pixels composing an image. Spatial domain methods are procedures that operate directly on these pixels. Spatial domain processes will be denoted by the expression

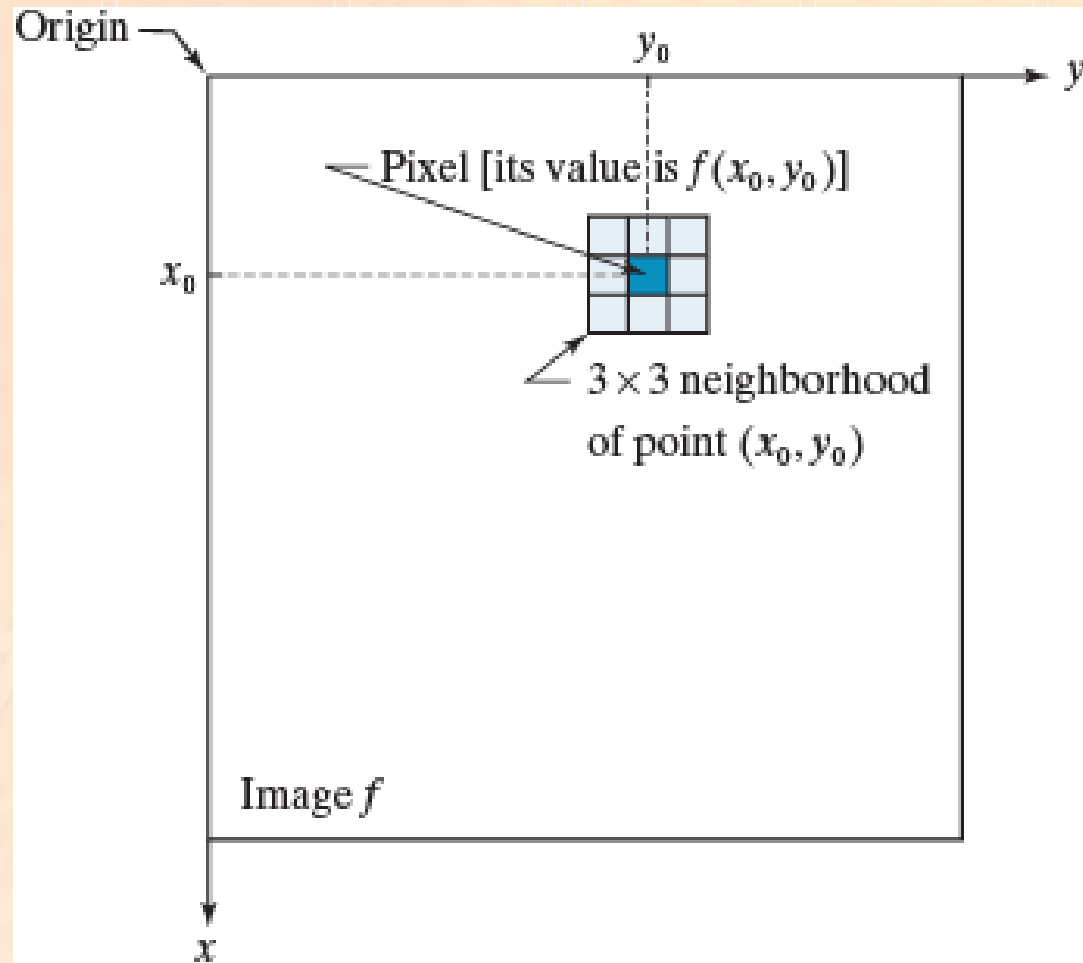
$$g(x, y) = T[f(x, y)] \quad (3.1-1)$$

where  $f(x, y)$  is the input image,  $g(x, y)$  is the processed image, and  $T$  is an operator on  $f$ , defined over some neighborhood of  $(x, y)$ .

- The principal approach in defining a neighborhood about a point  $(x, y)$  is to use a square or rectangular subimage area centered at  $(x, y)$ , as Fig. 3.1 shows.

**FIGURE 3.1**

A  $3 \times 3$  neighborhood about a point  $(x_0, y_0)$  in an image. The neighborhood is moved from pixel to pixel in the image to generate an output image. Recall from Chapter 2 that the value of a pixel at location  $(x_0, y_0)$  is  $f(x_0, y_0)$ , the value of the image at that location.

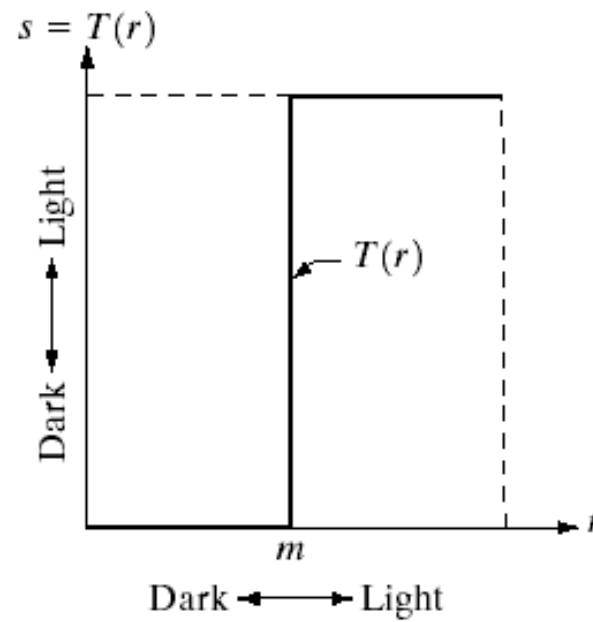
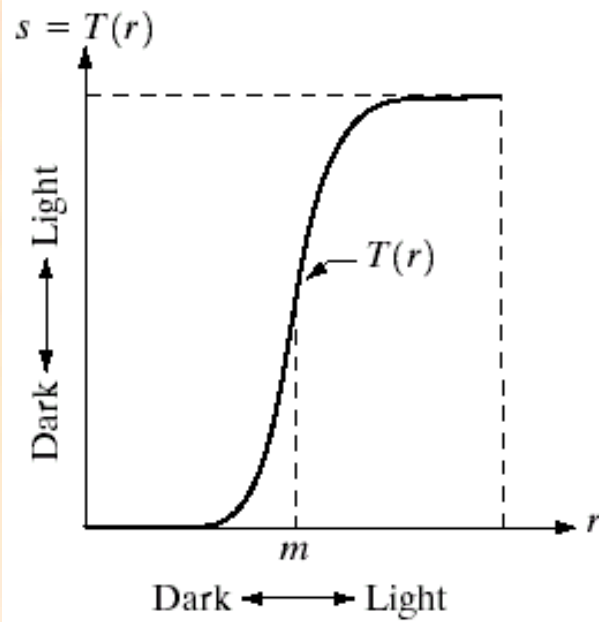


The simplest form of  $T$  is when the neighborhood is of size  $1 \times 1$  (that is, a single pixel). In this case,  $g$  depends only on the value of  $f$  at  $(x, y)$ , and  $T$  becomes a *gray-level* (also called an *intensity* or *mapping*) *transformation function* of the form

$$\underline{s = T(r)} \quad (3.1-2)$$

where, for simplicity in notation,  $r$  and  $s$  are variables denoting, respectively, the gray level of  $f(x, y)$  and  $g(x, y)$  at any point  $(x, y)$ .

- *contrast stretching* - Fig.3-2(a)
- *thresholding* - Fig.3-2(b)



a b

**FIGURE 3.2** Gray-level transformation functions for contrast enhancement.

- *Masks* (also referred to as *filters*, *kernels*, *templates*, or *windows*)
  - Use a function of the values of  $f$  in a predefined neighborhood of  $(x, y)$  to determine the value of  $g$  at  $(x, y)$ .
  - Basically, a mask is a small (say,  $3 \times 3$ ) 2-D array.

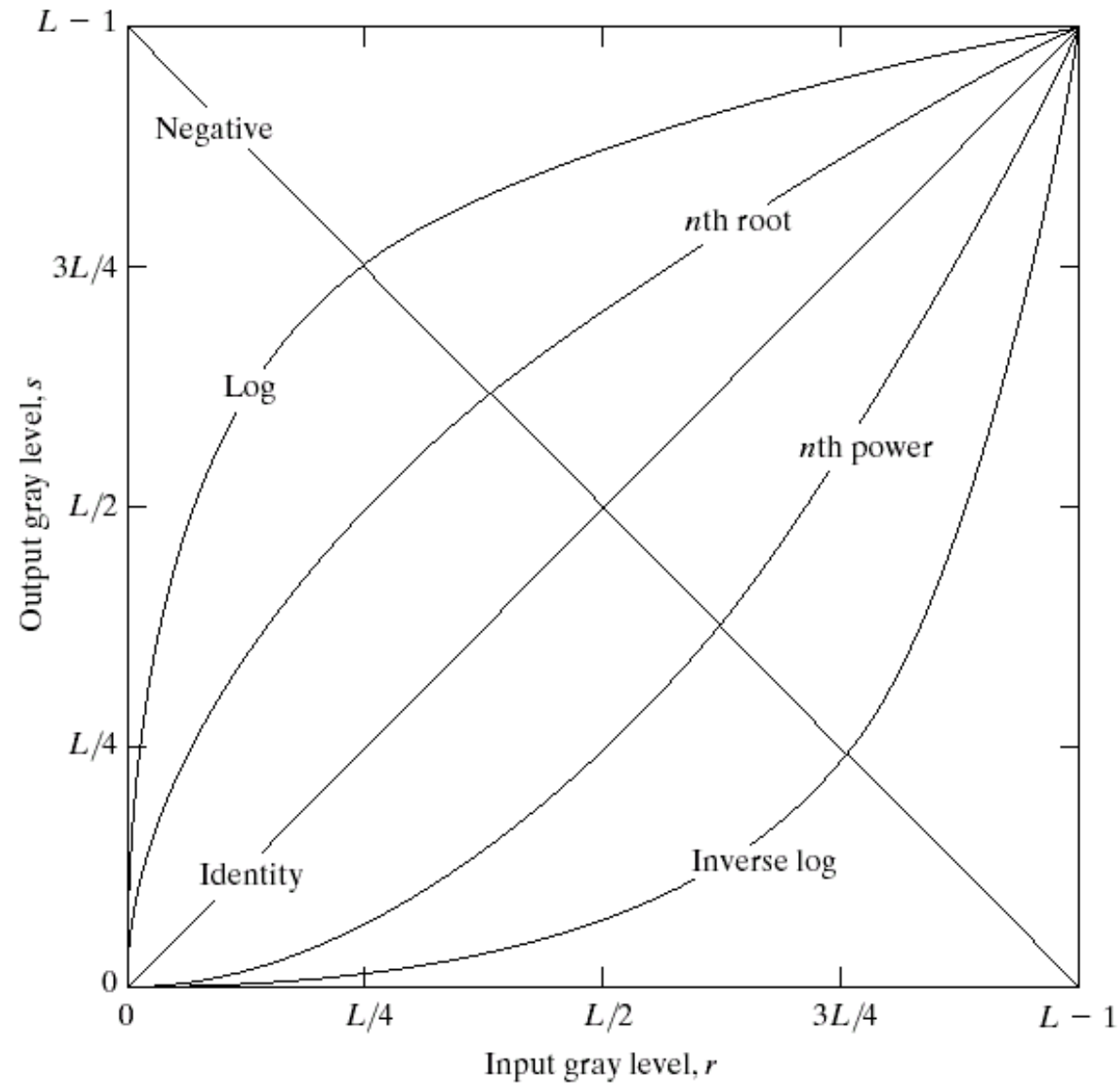


## 3.2 Some Basic Gray Level Transformations

- Three basic types of functions used frequently for image enhancement
  - Fig. 3.3
    - Linear (negative and identity transformations)
    - logarithmic (log and inverse-log transformations)
    - power-law ( $n$ th power and  $n$ th root transformations).



**FIGURE 3.3** Some basic gray-level transformation functions used for image enhancement.



- **Image Negatives**

$$s = L - I - r$$

- [Fig. 3.4.](#)

- **Log Transformations**

$$s = c \log (I + r)$$

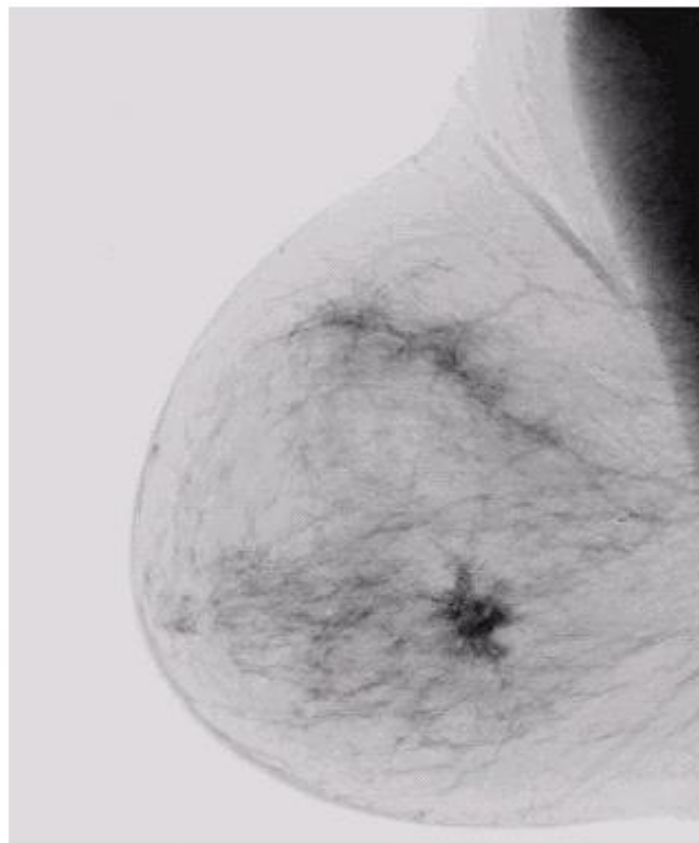
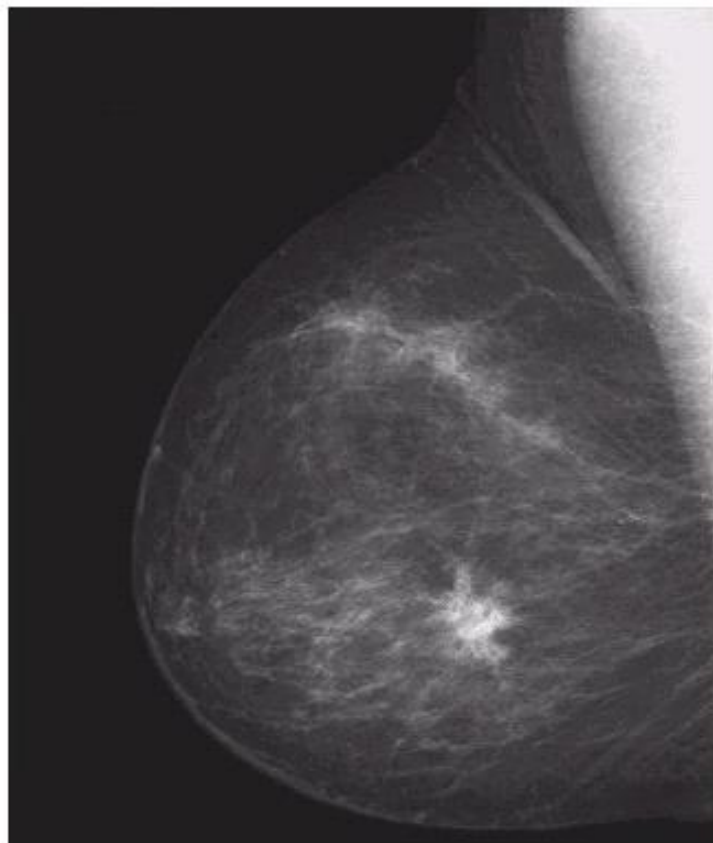
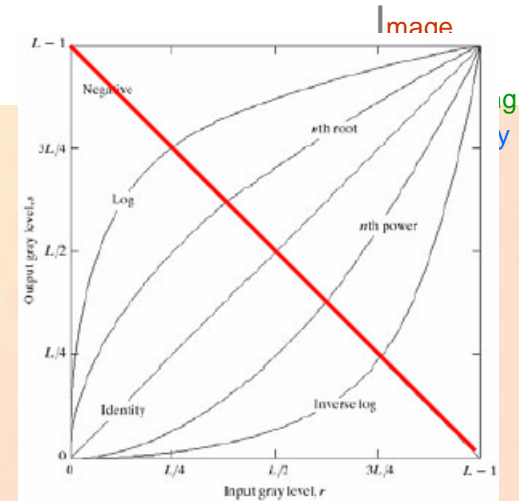
- [Fig. 3.5.](#)

- **Power-Law Transformations**

$$s = c r^r$$

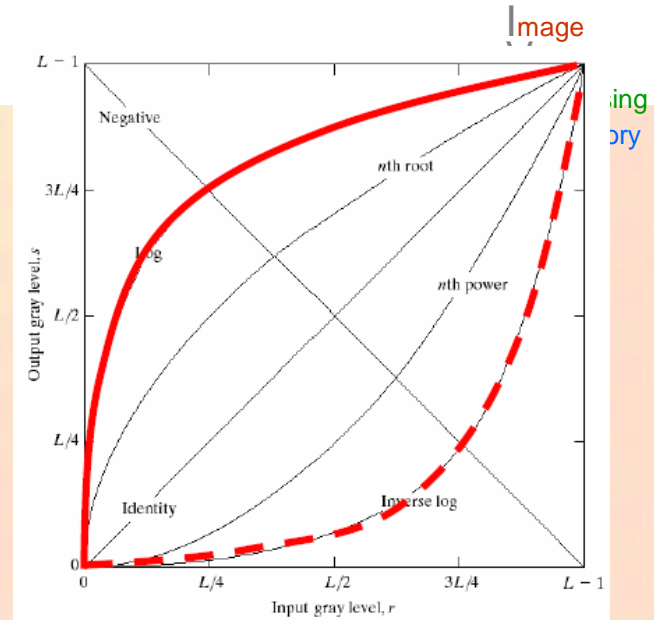
- Plots of  $s$  versus  $r$  for various values of  $r$  are shown in [Fig. 3.6.](#)
- Cathode ray tube (CRT) devices example in [Fig. 3.7.](#)

$$s = T(r) = (L-1) - r$$



**a b**  
**FIGURE 3.4**  
 (a) Original digital mammogram.  
 (b) Negative image obtained using the negative transformation in Eq. (3.2-1).  
 (Courtesy of G.E. Medical Systems.)

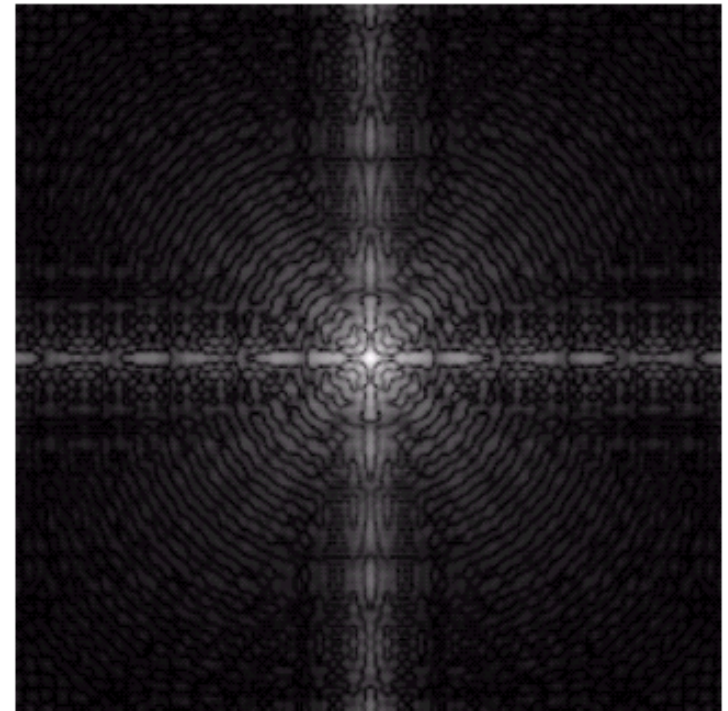
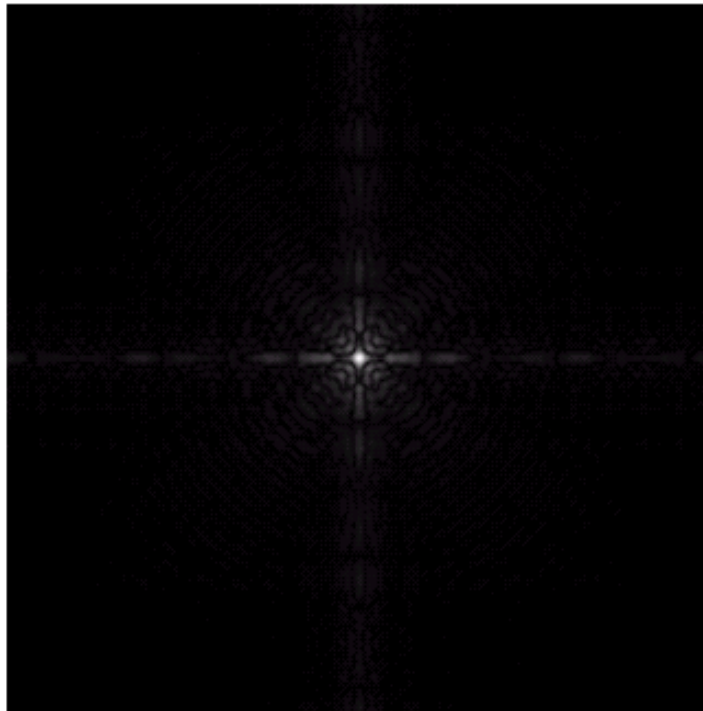
Value in the range 0 to  $1.5 \times 10^6$



a b

### FIGURE 3.5

- (a) Fourier spectrum.
- (b) Result of applying the log transformation given in Eq. (3.2-2) with  $c = 1$ .



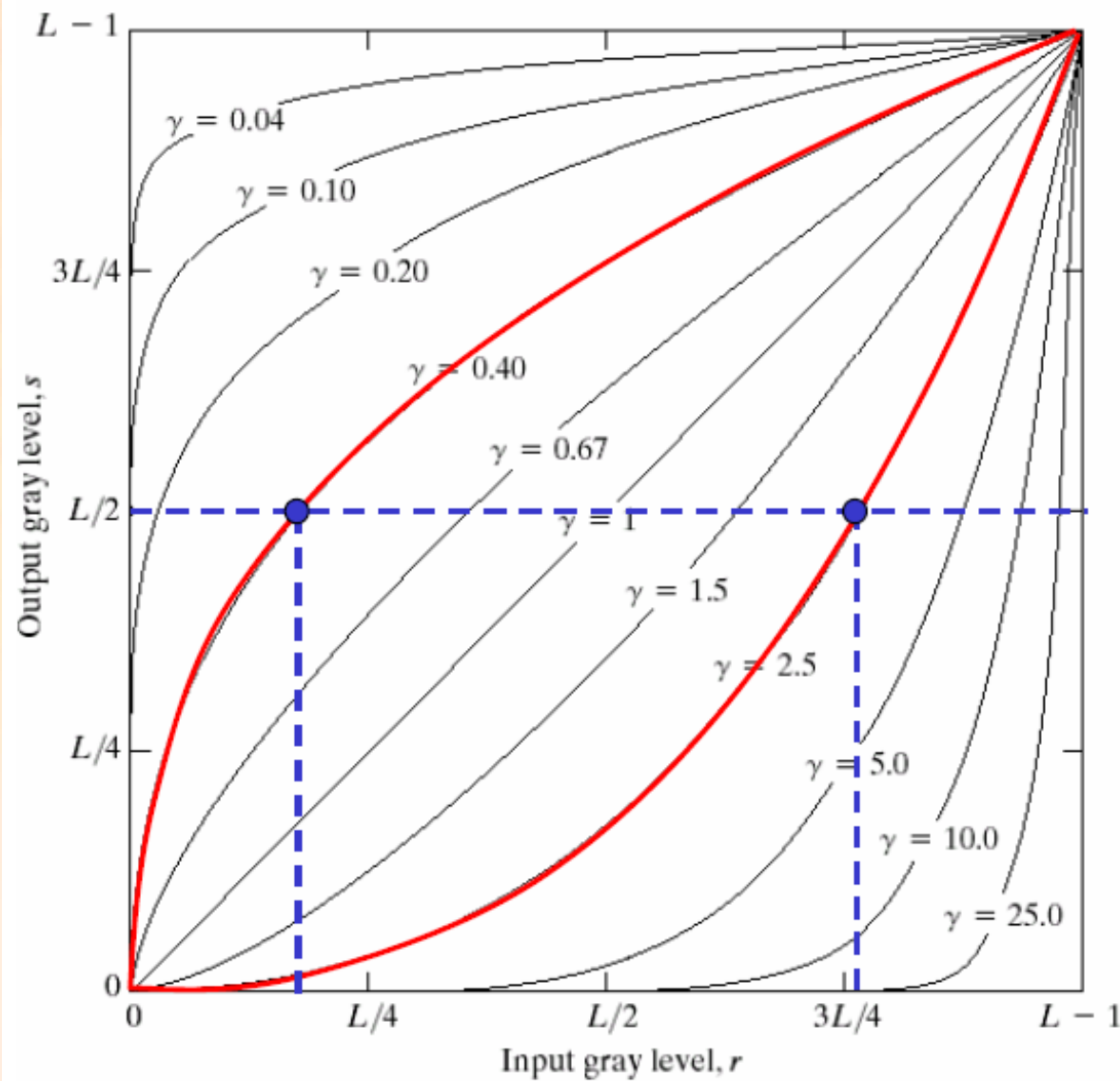


**FIGURE 3.6** Plots of the equation  $s = cr^\gamma$  for various values of  $\gamma$  ( $c = 1$  in all cases).



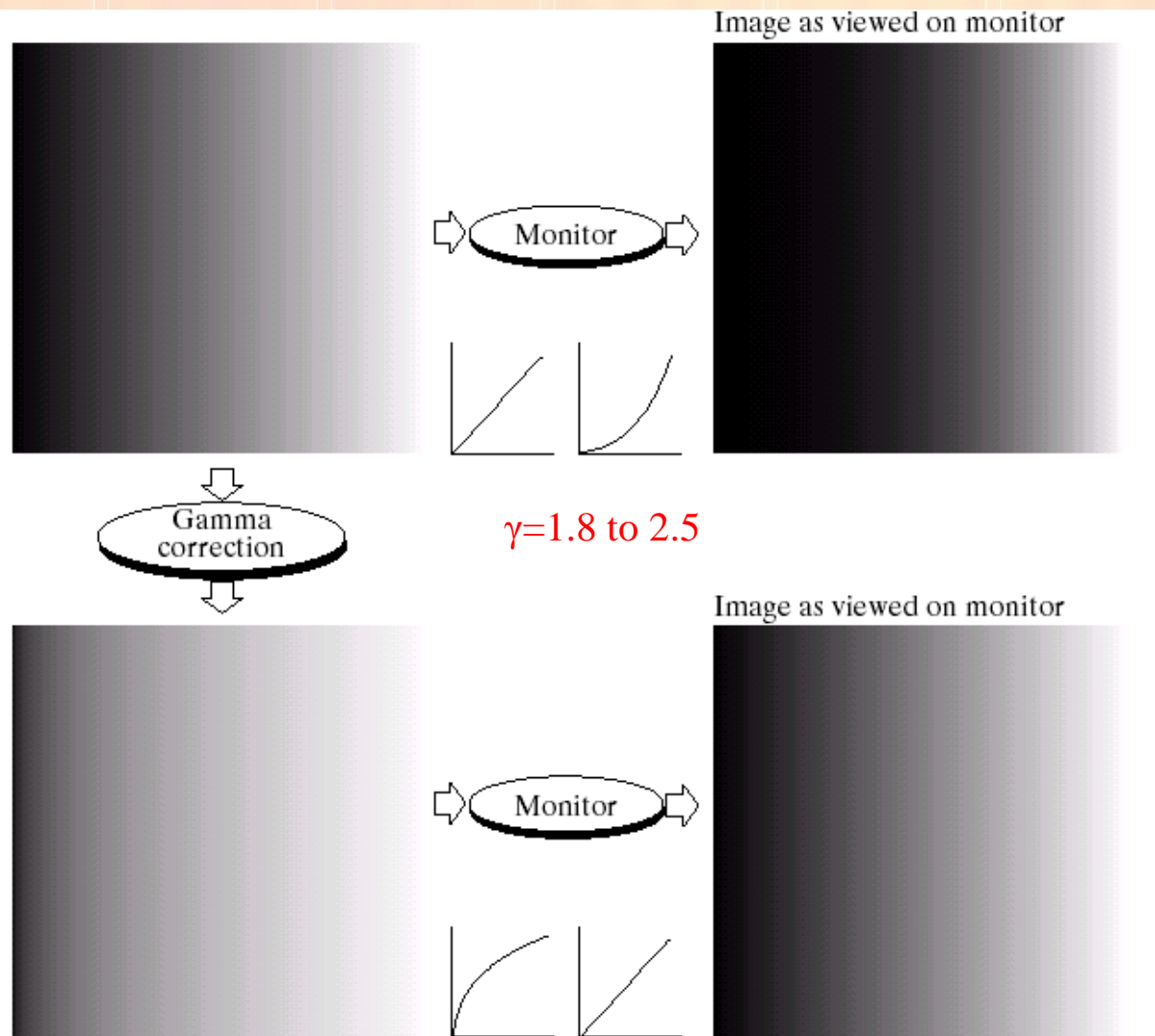
# Gamma correction

$$s = T(r) = cr^\gamma$$

a b  
c d

**FIGURE 3.7**

(a) Linear-wedge gray-scale image.  
(b) Response of monitor to linear wedge.  
(c) Gamma-corrected wedge.  
(d) Output of monitor.



$\gamma=1.8 \text{ to } 2.5$

$\gamma=1/2.5$

- **EXAMPLE 3.1** Magnetic resonance (MR) image transformations

a	b
c	d

**FIGURE 3.8**

(a) Magnetic resonance image (MRI) of a fractured human spine (the region of the fracture is enclosed by the circle).

(b)–(d) Results of applying the transformation in Eq. (3-5) with  $c = 1$  and  $\gamma = 0.6, 0.4$ , and  $0.3$ , respectively. (Original image courtesy of Dr. David R. Pickens, Department of Radiology and Radiological Sciences, Vanderbilt University Medical Center.)

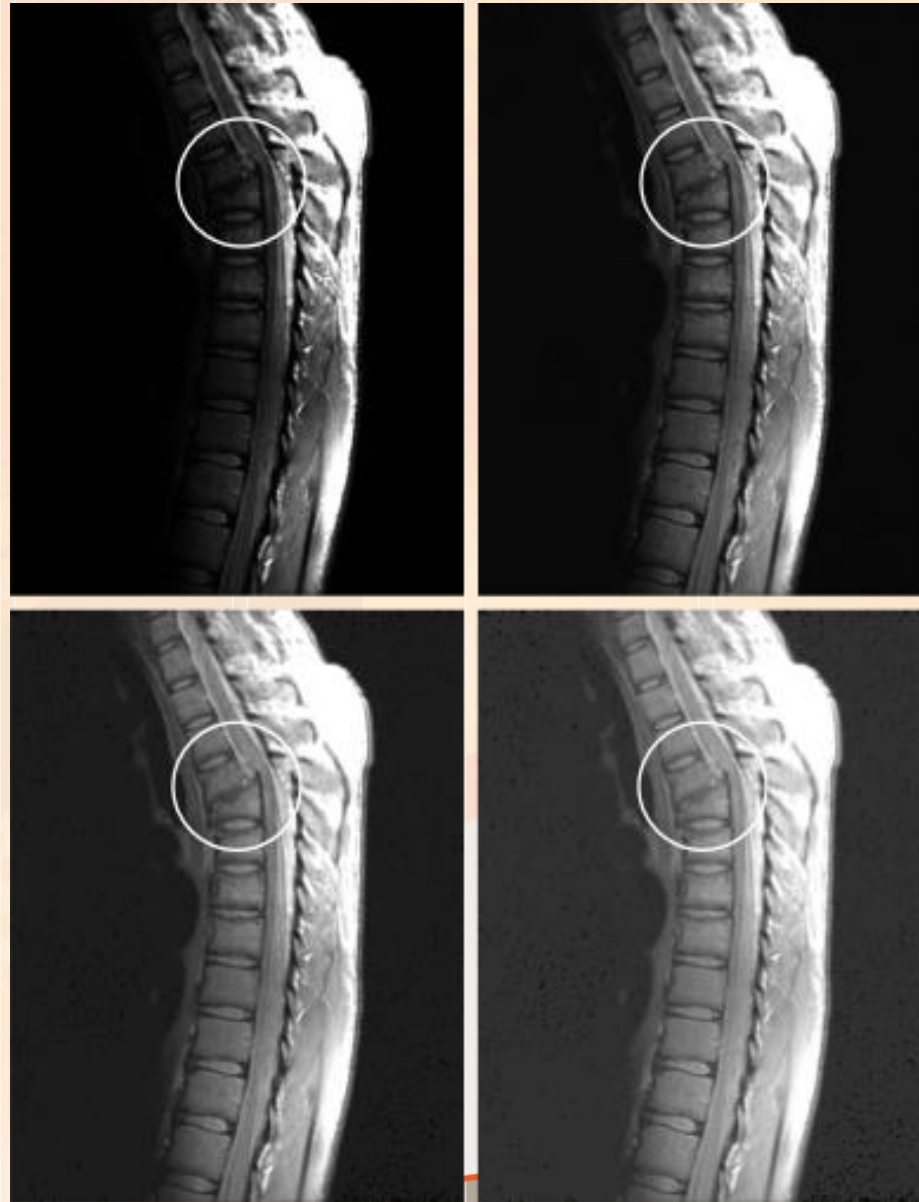




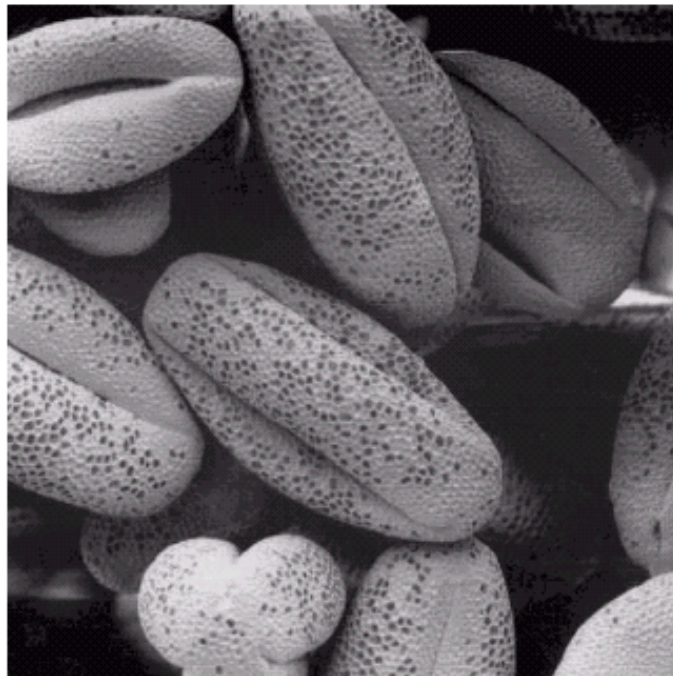
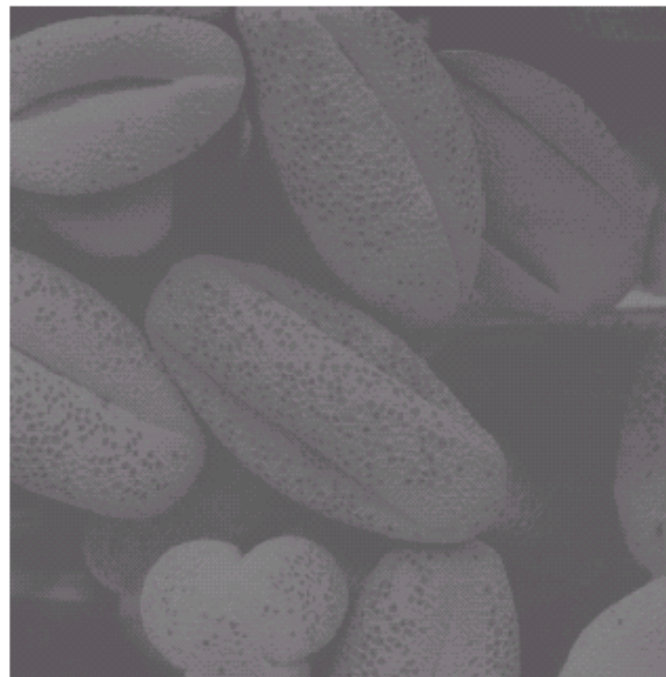
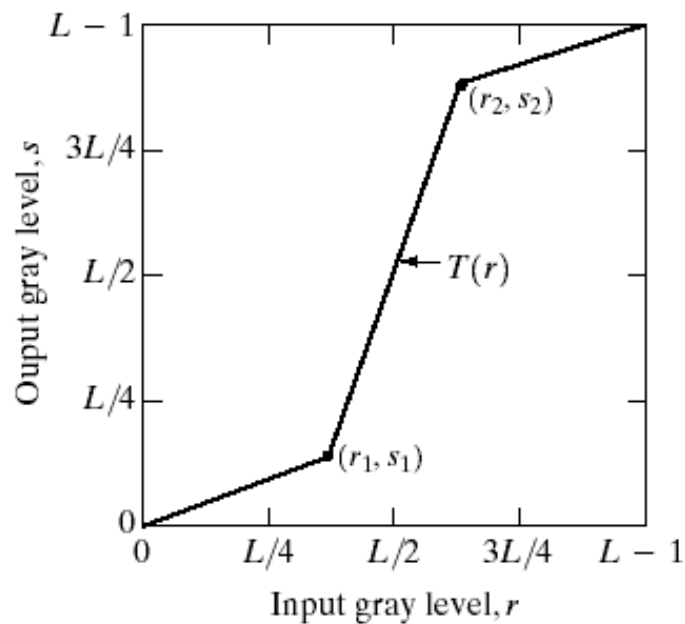
Image  
Video  
Processing  
Laboratory

(a) Aerial image.  
(b)–(d) Results of applying the transformation in Eq. (3.2-3) with  $c = 1$  and  $\gamma = 3.0, 4.0$ , and  $5.0$ , respectively. (Original image for this example courtesy of NASA.)



- **Piecewise-Linear Transformation Functions**
  - **Contrast stretching**
    - [Figure 3.10](#)
  - **Gray-level slicing**
    - [Figure 3.11](#)
  - **Bit-plane slicing**
    - [Figure 3.12](#)
    - [Figure 3.13](#)
    - [Figure 3.14](#)



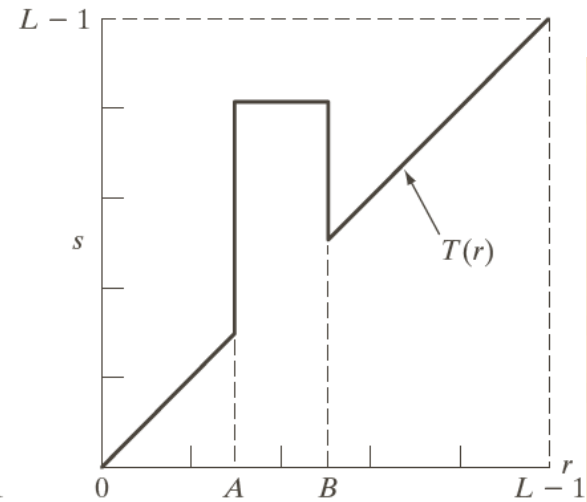
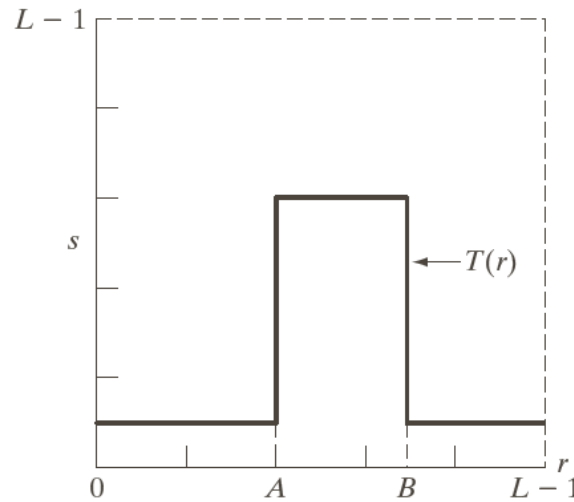


a b  
c d

**FIGURE 3.10**  
Contrast stretching.  
(a) Form of transformation function. (b) A low-contrast image. (c) Result of contrast stretching. (d) Result of thresholding. (Original image courtesy of Dr. Roger Heady, Research School of Biological Sciences, Australian National University, Canberra, Australia.)

a b

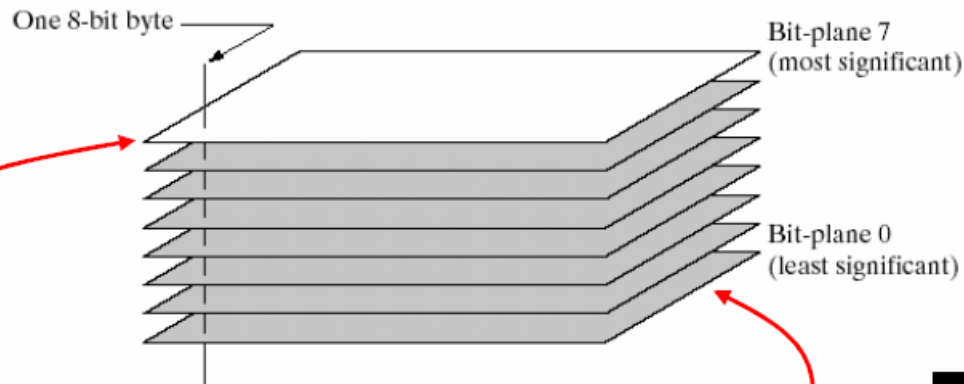
**FIGURE 3.11** (a) This transformation highlights intensity range  $[A, B]$  and reduces all other intensities to a lower level. (b) This transformation highlights range  $[A, B]$  and preserves all other intensity levels.



a b c

**FIGURE 3.12** (a) Aortic angiogram. (b) Result of using a slicing transformation of the type illustrated in Fig. 3.11(a), with the range of intensities of interest selected in the upper end of the gray scale. (c) Result of using the transformation in Fig. 3.11(b), with the selected area set to black, so that grays in the area of the blood vessels and kidneys were preserved. (Original image courtesy of Dr. Thomas R. Gest, University of Michigan Medical School.)

# ✓ Bit-plane slicing



$$170 = 1 \times 2^7 + 0 \times 2^6 + 1 \times 2^5 + 0 \times 2^4 + 1 \times 2^3 + 0 \times 2^2 + 1 \times 2^1 + 0 \times 2^0$$

$$255 = 1 \times 2^7 + 1 \times 2^6 + 1 \times 2^5 + 1 \times 2^4 + 1 \times 2^3 + 1 \times 2^2 + 1 \times 2^1 + 1 \times 2^0$$

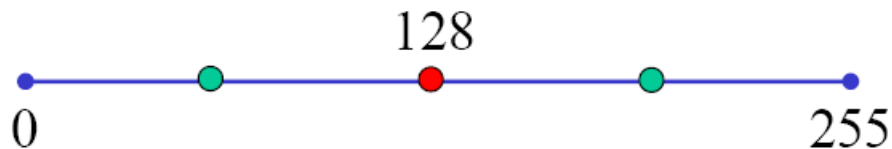


**FIGURE 3.12**  
Bit-plane  
representation of  
an 8-bit image.

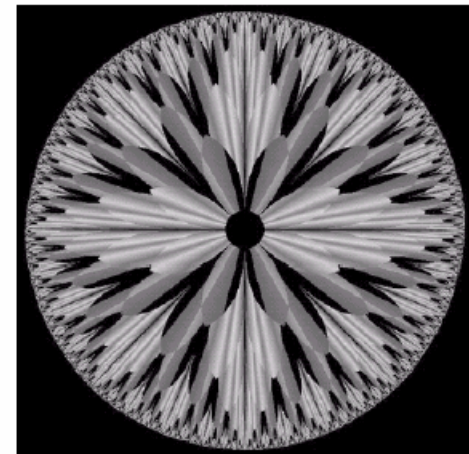


**FIGURE 3.13** An 8-bit fractal image. (A fractal is an image generated from mathematical expressions). (Courtesy of Ms. Melissa D. Binde, Swarthmore College, Swarthmore, PA.)



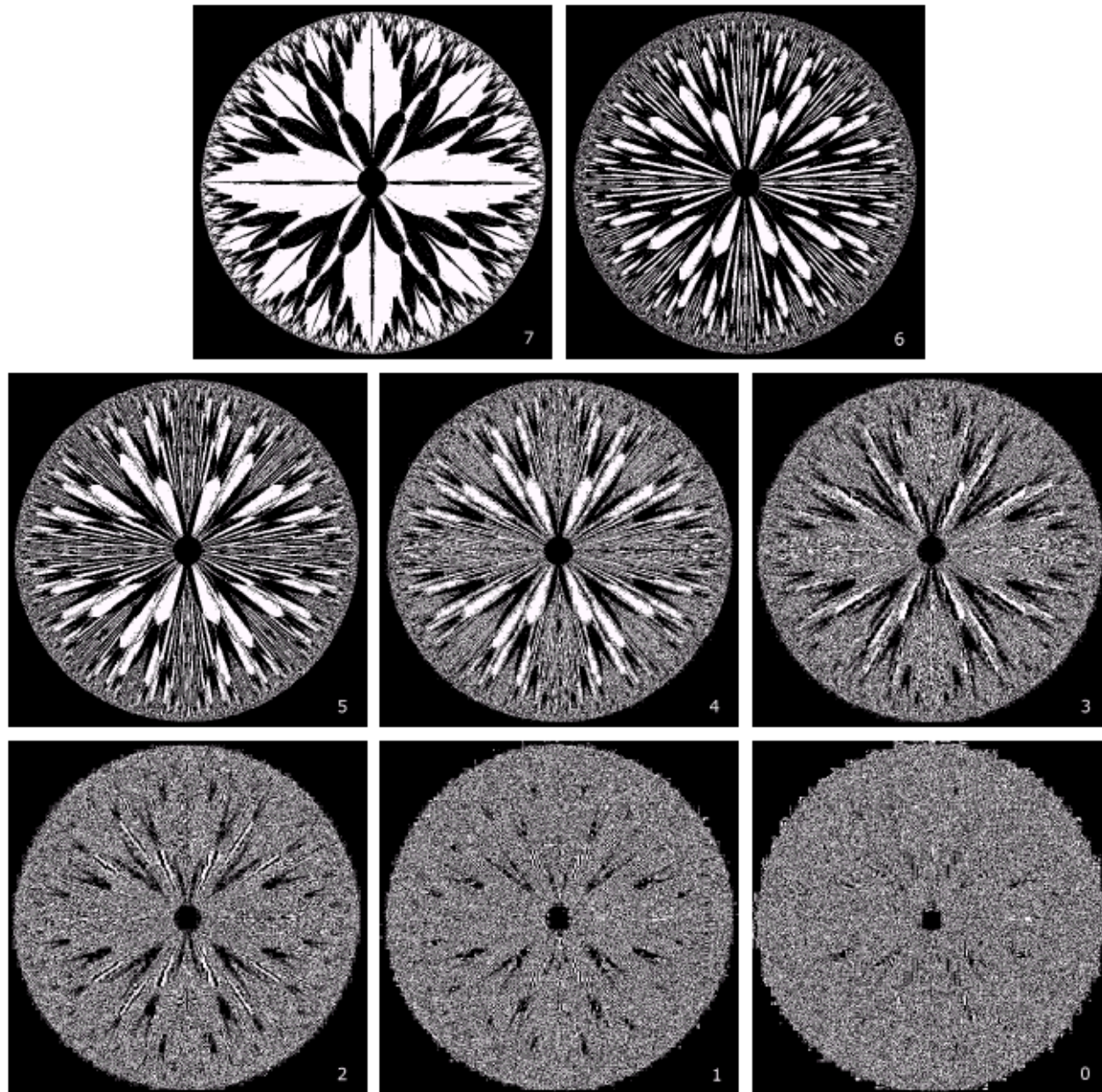
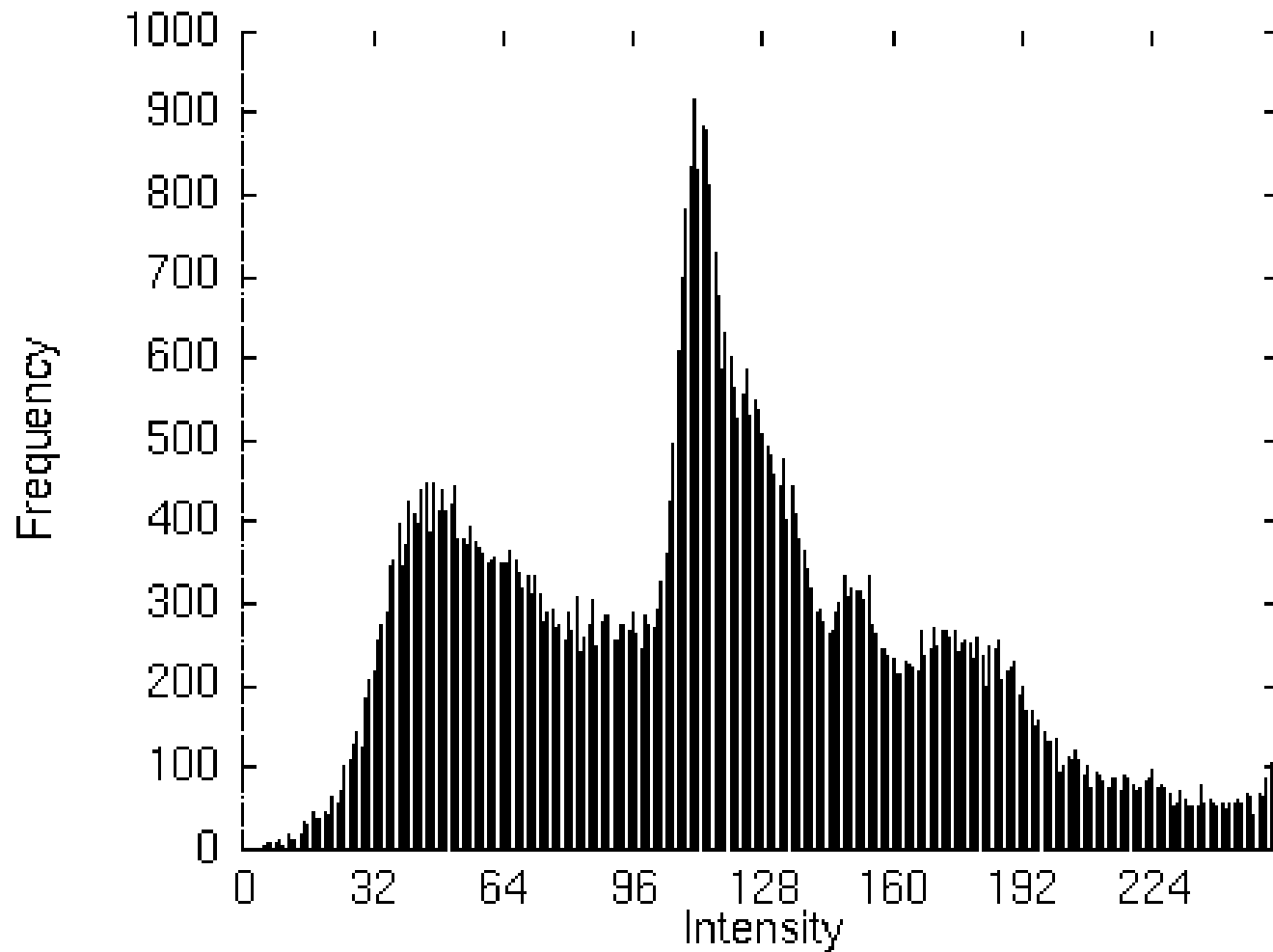


**FIGURE 3.14** The eight bit planes of the image in Fig. 3.13. The number at the bottom, right of each image identifies the bit plane.

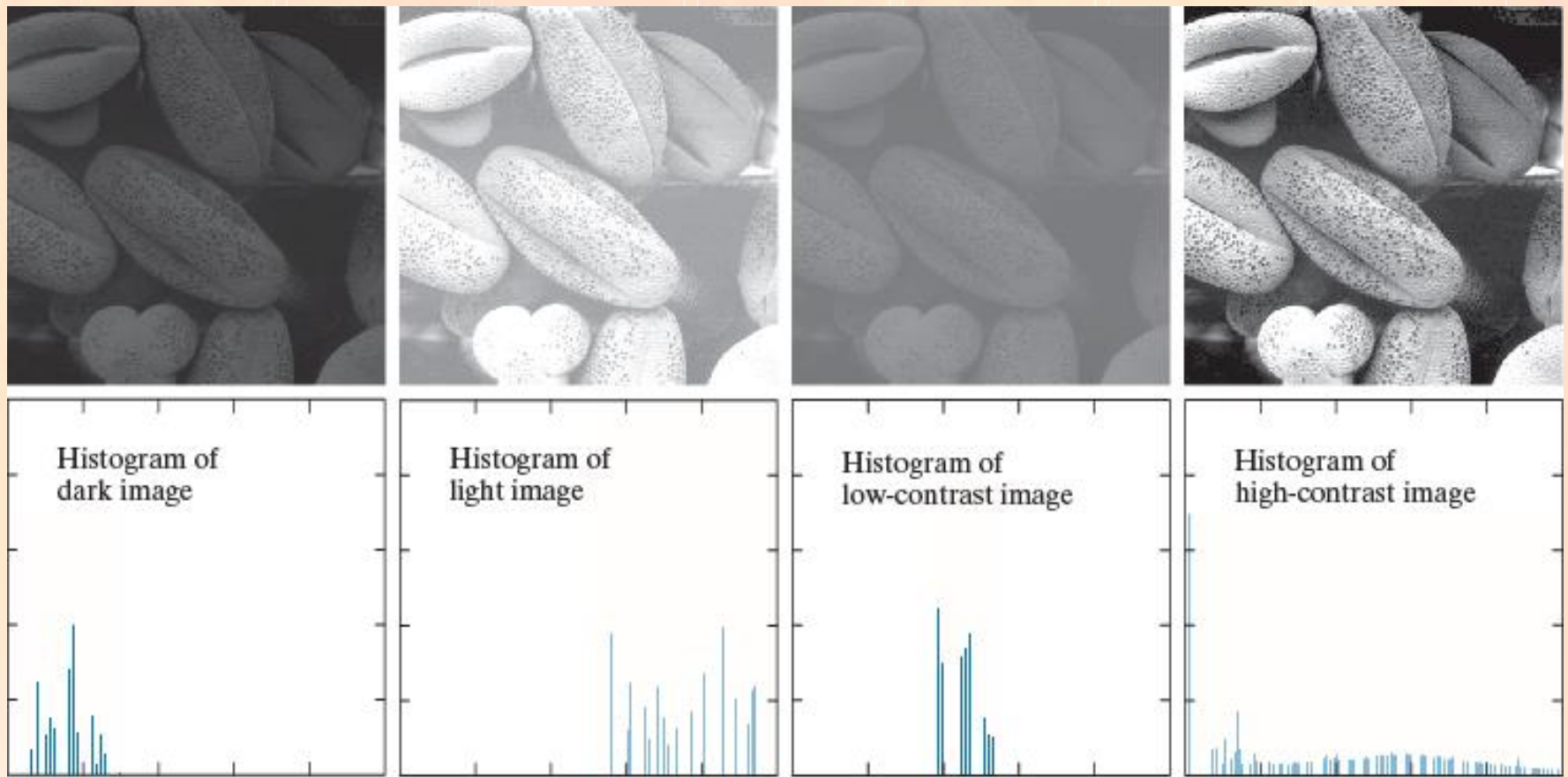
# 3.3 Histogram Processing

- The histogram of a digital image with gray levels in the range  $[0, L-1]$  is a discrete function  $h(r_k)=n_k$ , where  $r_k$  is the  $k$ th gray level and  $n_k$  is the number of pixels in the image having gray level  $r_k$ .
- Histograms are the basis for numerous spatial domain processing techniques.
- Histogram manipulation can be used effectively for image enhancement.
  - histograms corresponding to images in Fig. 3-15.





*A brightness histogram.*

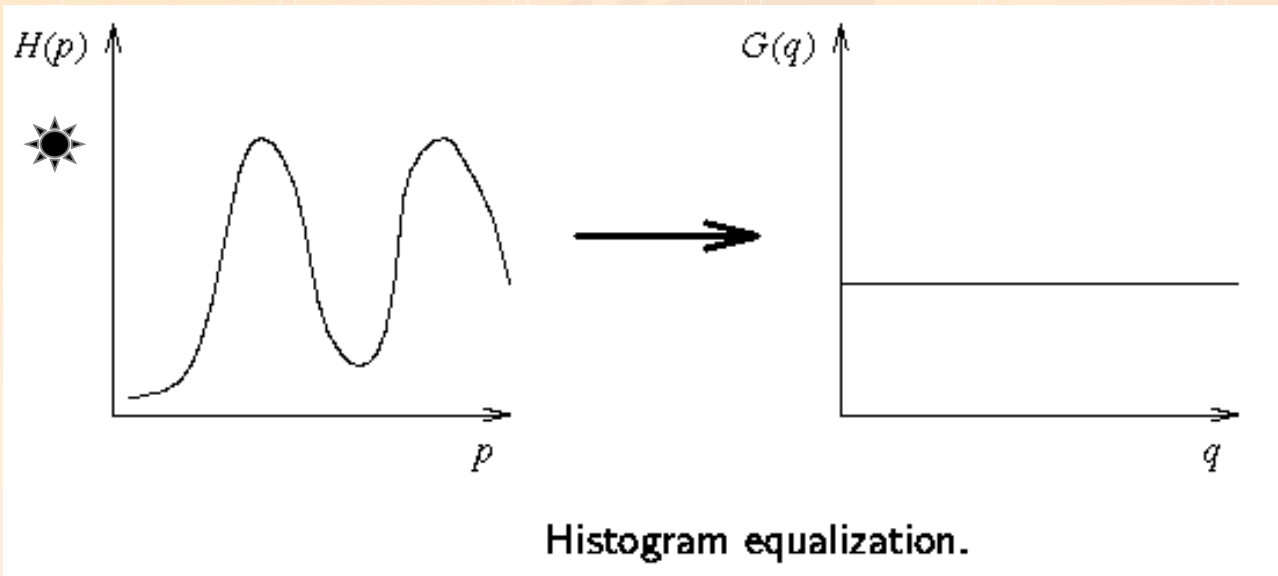


a b c d

**FIGURE 3.16** Four image types and their corresponding histograms. (a) dark; (b) light; (c) low contrast; (d) high contrast. The horizontal axis of the histograms are values of  $r_k$  and the vertical axis are values of  $p(r_k)$ .

- **Histogram Equalization**

- The aim - image with equally distributed brightness levels over the whole brightness scale



# Histogram Equalization

- Foundation

Let  $r$  represent the normalized gray level of the pixels in the image to be enhanced, with

$$0 \leq r \leq 1$$

*(black)*                      *(white)*

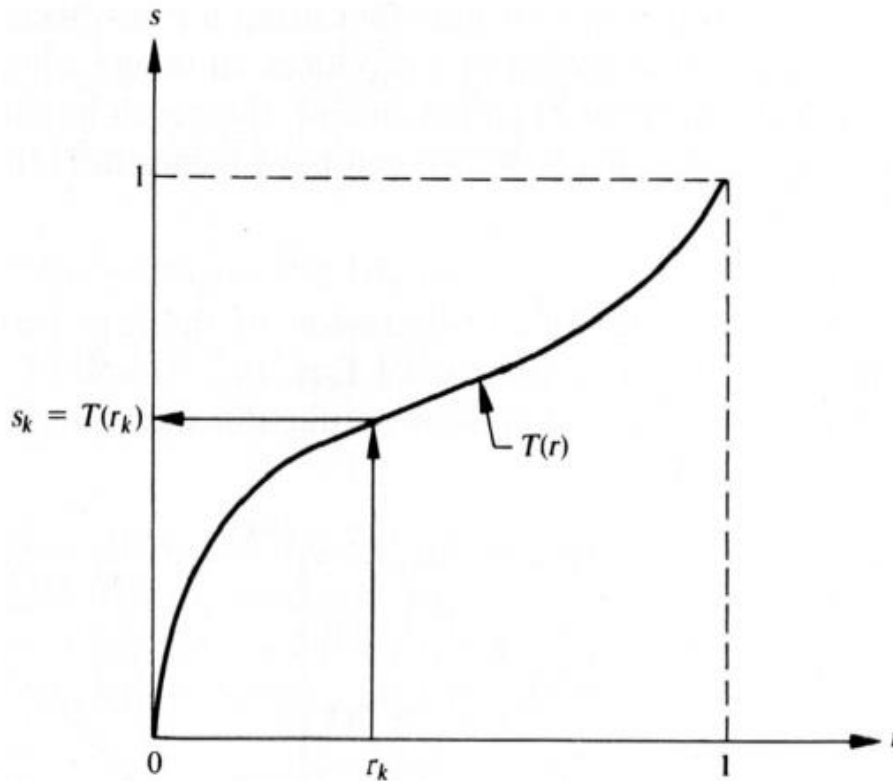
Transformations of the form

$$s = T(r)$$

will produce a level  $s$  for every pixel value  $r$  in the original image. It is assumed that

(a)  $T(r)$  is single-valued and monotonically increasing in the interval  $0 \leq r \leq 1$ ,

(b)  $0 \leq T(r) \leq 1$  for  $0 \leq r \leq 1$



The inverse transformation

$$r = T^{-1}(s)$$

is also assumed to satisfy  
cond. (a) and (b)

a b

**FIGURE 3.17**

(a) Monotonic increasing function, showing how multiple values can map to a single value. (b) Strictly monotonic increasing function. This is a one-to-one mapping, both ways.

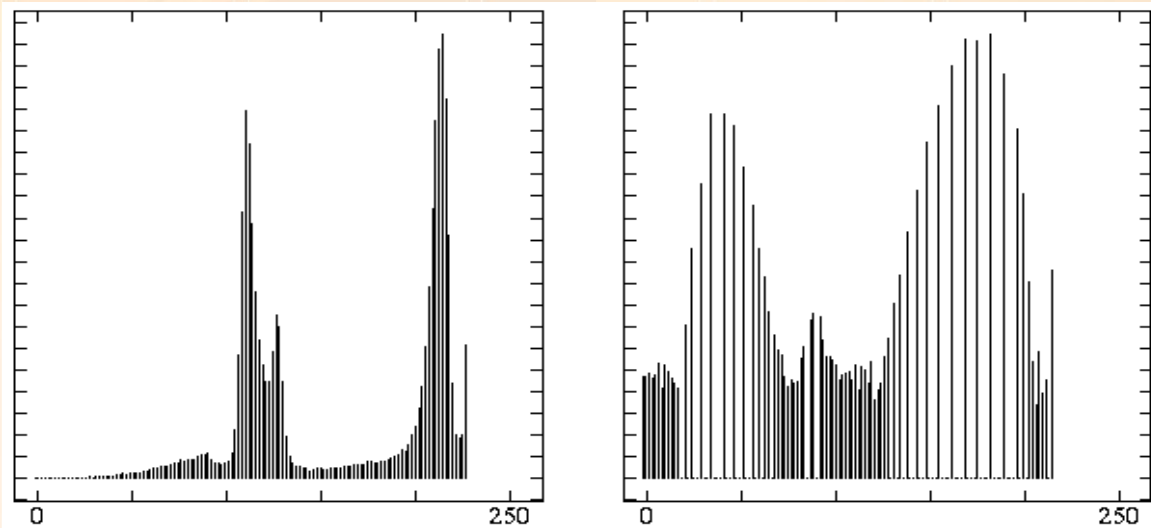
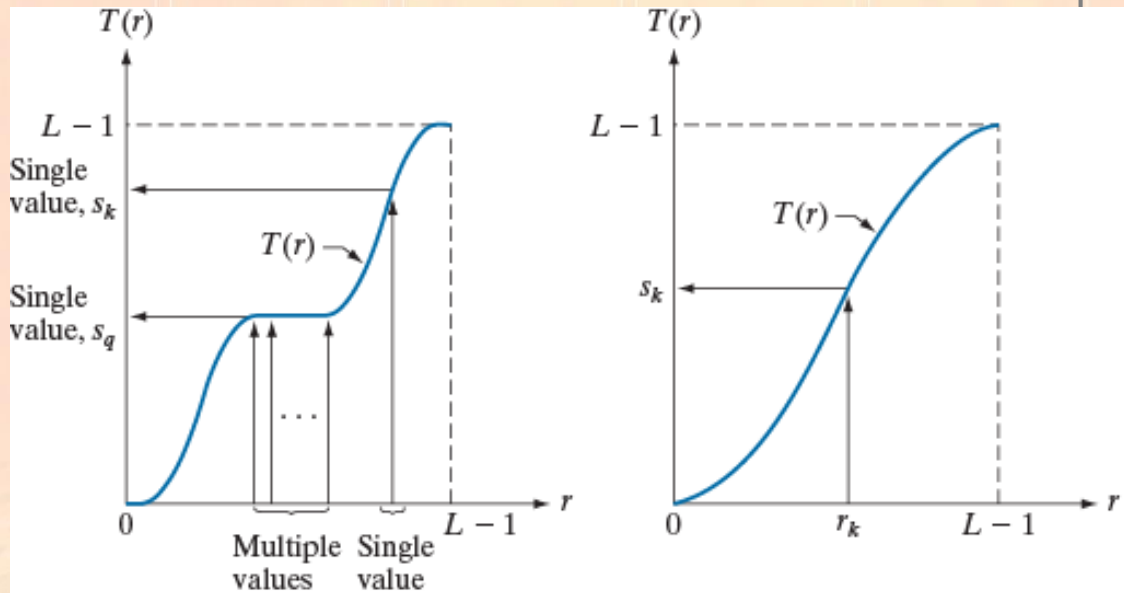
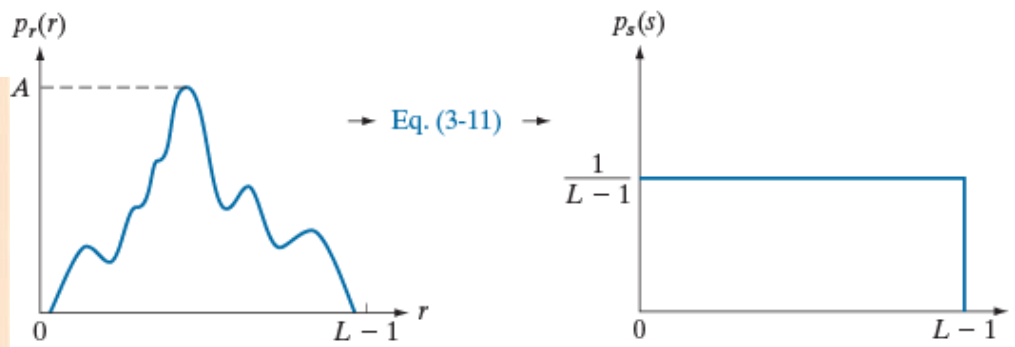


**Figure 4.4** Histogram equalization: Original and equalized histograms.





From probability theory, the p.d.f. of the transformed gray levels is given by

$$p_s(s) = \left[ p_r(r) \frac{dr}{ds} \right]_{r=T^{-1}(s)} \quad (1)$$

Now, consider the transformation function

$$s = T(r) = \int_0^r p_r(w) dw \quad 0 \leq r \leq 1 \quad (2)$$

$$\frac{ds}{dr} = p_r(r)$$

Subst. into Eq. (1)

$$p_s(s) = \left[ p_r(r) \frac{1}{p_r(r)} \right]_{r=T^{-1}(s)} = [1]_{r=T^{-1}(s)} = 1 \quad 0 \leq s \leq 1$$



From probability theory, the p.d.f. of the transformed gray levels is given by

$$p_r(r_k) = \left[ \frac{n_k}{n} \right] \quad 0 \leq r_k \leq 1 \text{ and } k = 0, 1, \dots, L-1$$

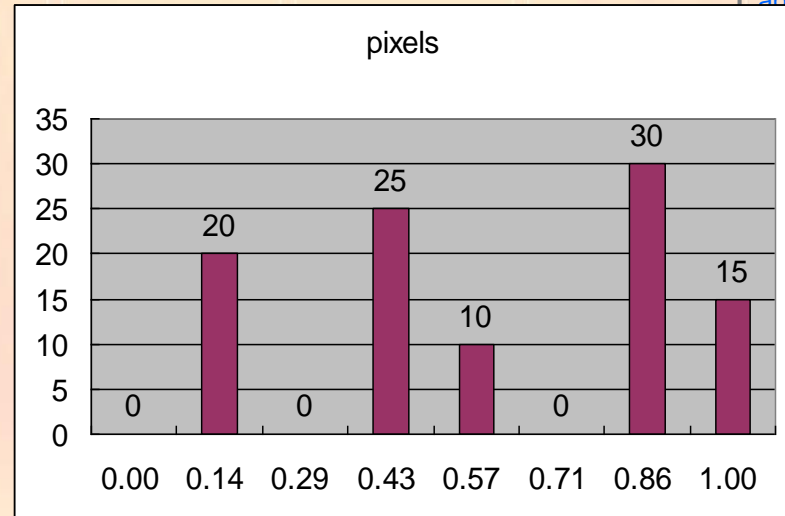
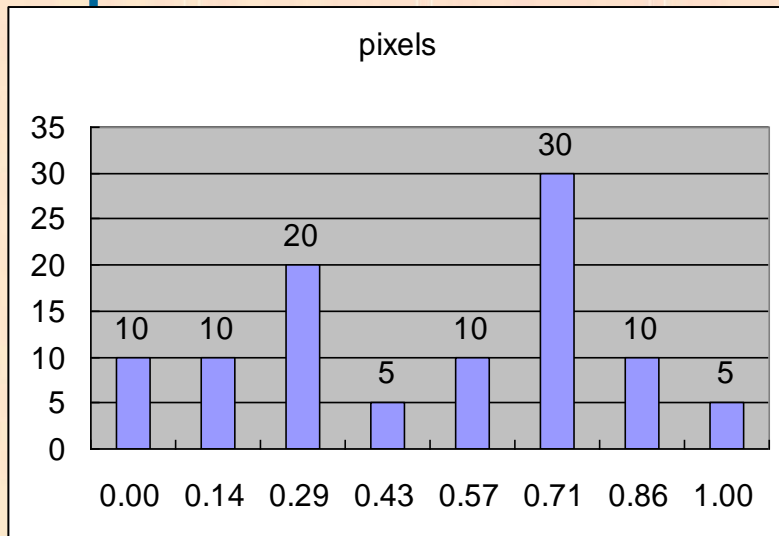
The discrete form of *Eq. (2)* is given by

$$s_k = T(r_k) = \sum_{j=0}^k \frac{n_j}{n} = \sum_{j=0}^k p_r(r_j) \quad 0 \leq r_k \leq 1 \text{ and } k = 0, 1, \dots, L-1$$

The inverse transform is denoted by

$$r_k = T^{-1}(s_k) \quad 0 \leq s_k \leq 1$$

# Example



Gray-level	0	1	2	3	4	5	6	7
$r$	0.00	0.14	0.29	0.43	0.57	0.71	0.86	1.00
$pixels$	10	10	20	5	10	30	10	5
$pr$	0.1	0.1	0.2	0.05	0.1	0.3	0.1	0.05
$sk$	0.1	0.2	0.4	0.45	0.55	0.85	0.95	1
$r'$	0.14	0.14	0.43	0.43	0.57	0.86	1.00	1.00

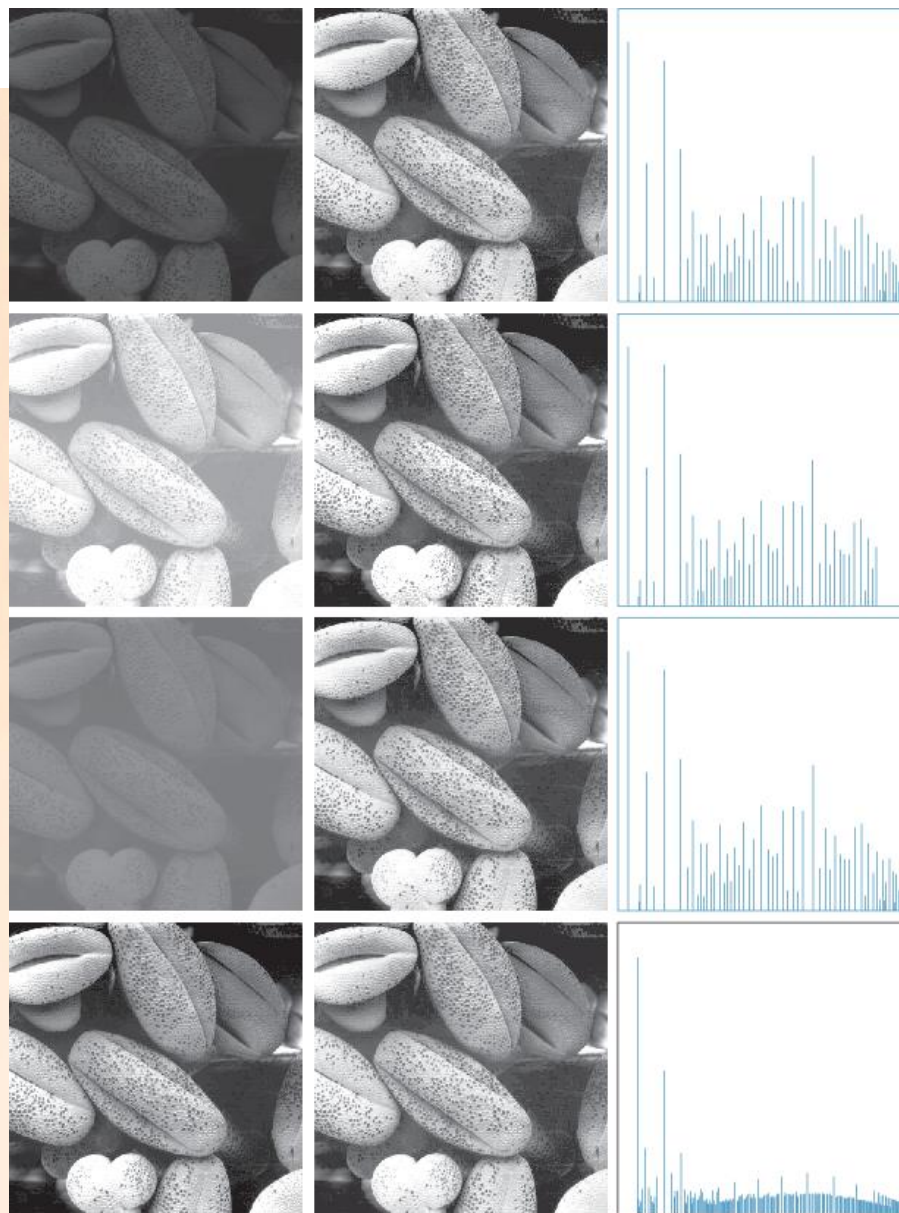


**FIGURE 3.20** Left column: Images from Fig. 3.16. Center column: Corresponding histogram-equalized images. Right column: histograms of the images in the center column (compare with the histograms in Fig. 3.16).

# Direct Histogram Specification

Suppose that a given image is first histogram equalized using

$$s = T(r) = \int_0^r p_r(w)dw \quad (1)$$

If the desired image were available, its levels could also be equalized by using the transformation function

$$v = G(z) = \int_0^z p_z(w)dw \quad (2)$$

The inverse process,  $z = G^{-1}(v)$ , would then yield the desired levels back.

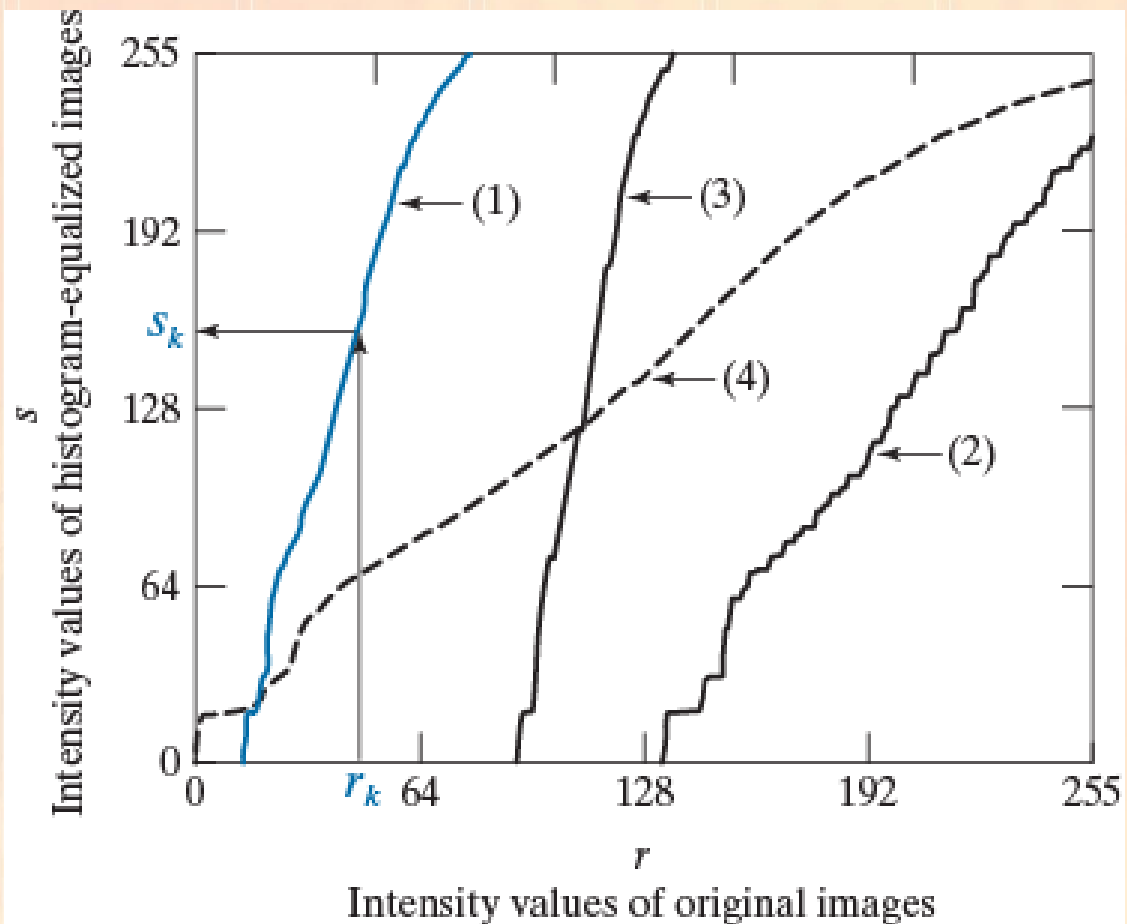
*The procedure can be summarized as follows:*

- (1) Equalize the levels of the original image using *Eq. (1)*,
- (2) Specify the desired density function and obtain the transformation  $G(z)$  using *Eq. (2)*,
- (3) Apply the inverse transformation function,  $z = G^{-1}(s)$ , to the levels obtained in step (1).



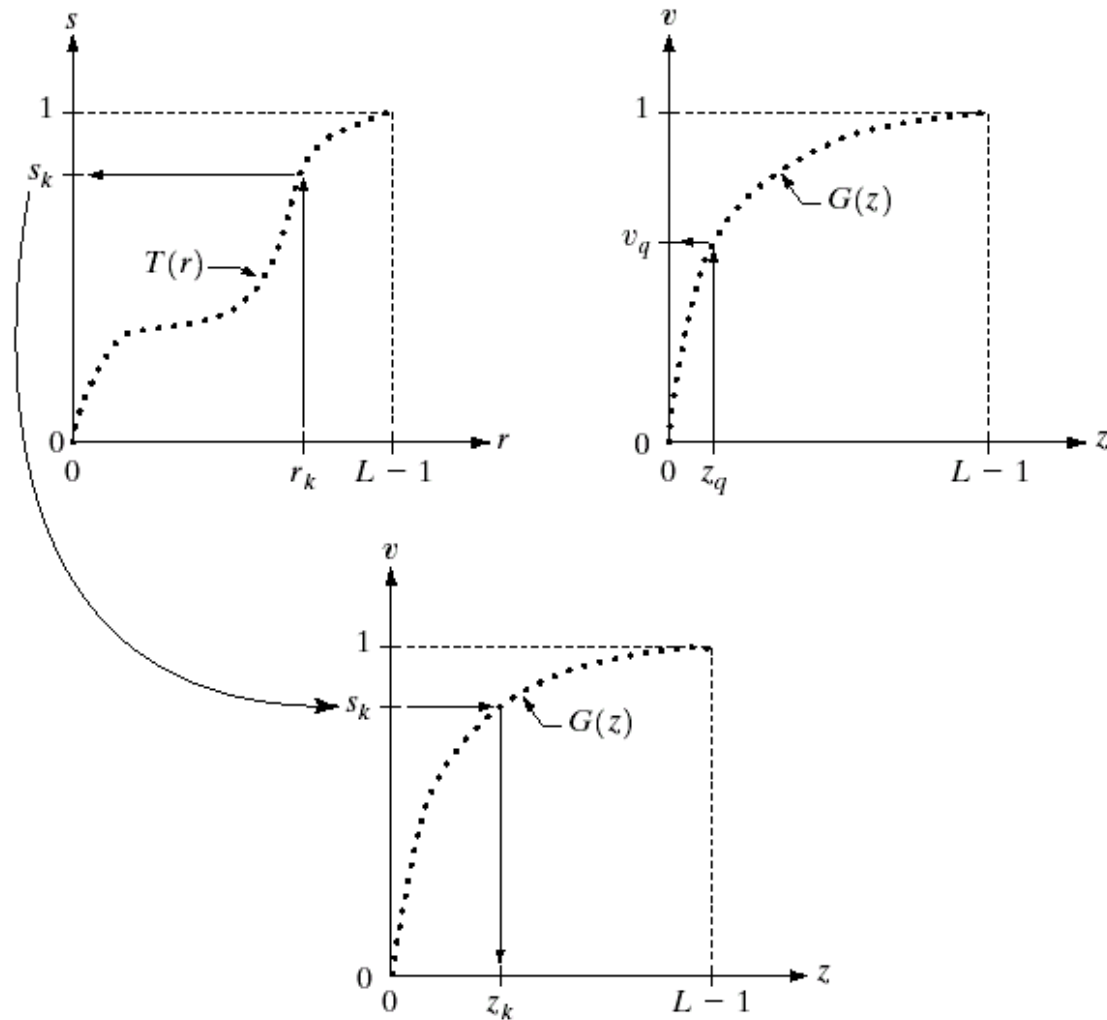
**FIGURE 3.21**

Transformation functions for histogram equalization. Transformations (1) through (4) were obtained using Eq. (3-15) and the histograms of the images on the left column of Fig. 3.20. Mapping of one intensity value  $r_k$  in image 1 to its corresponding value  $s_k$  is shown.

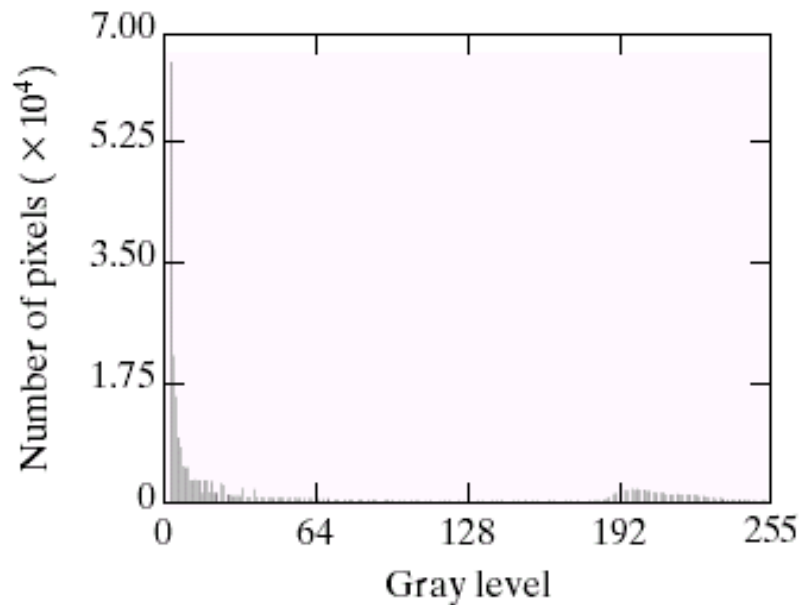
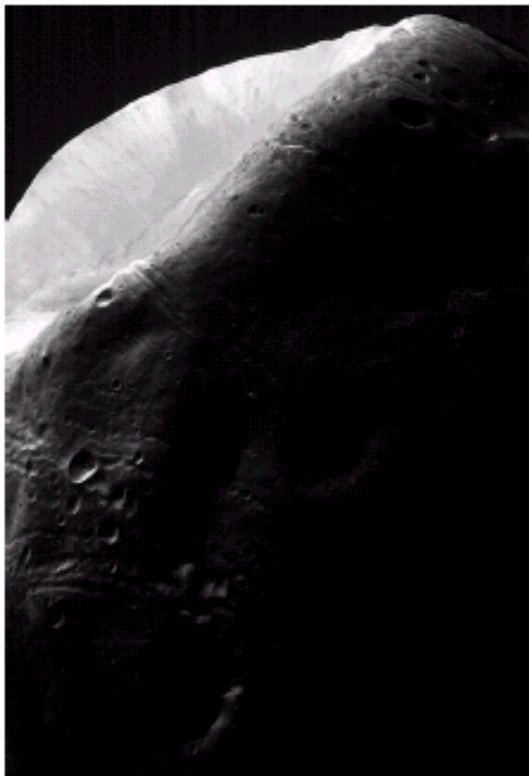


a b  
c**FIGURE 3.19**

(a) Graphical interpretation of mapping from  $r_k$  to  $s_k$  via  $T(r)$ .  
(b) Mapping of  $z_q$  to its corresponding value  $v_q$  via  $G(z)$ .  
(c) Inverse mapping from  $s_k$  to its corresponding value of  $z_k$ .

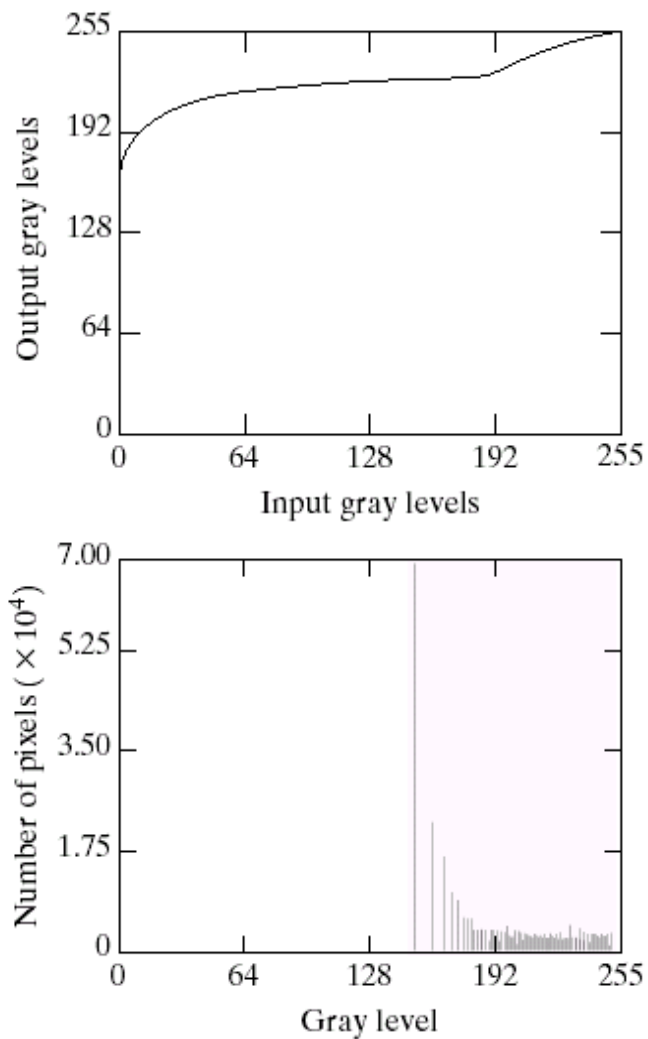






a b

**FIGURE 3.20** (a) Image of the Mars moon Phobos taken by NASA's *Mars Global Surveyor*. (b) Histogram. (Original image courtesy of NASA.)



a b  
c

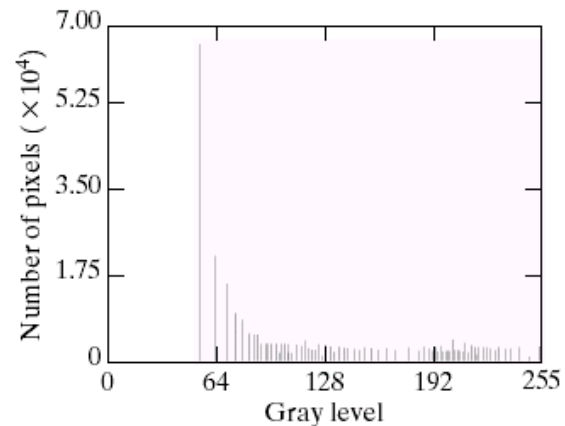
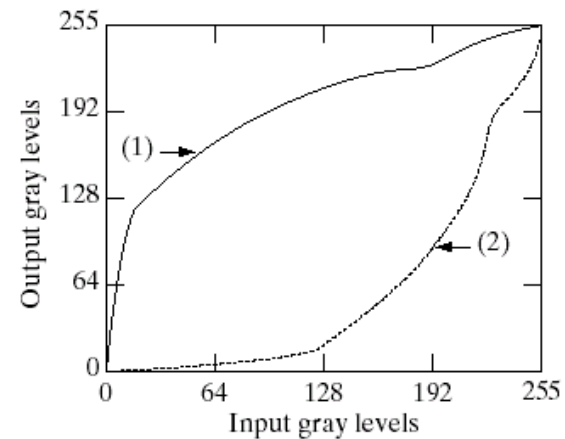
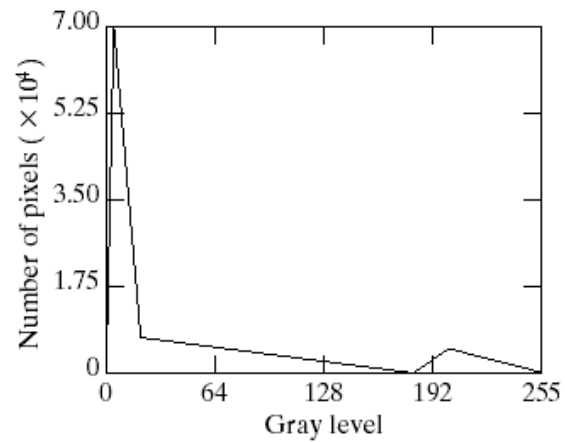
**FIGURE 3.21**

(a) Transformation function for histogram equalization.  
(b) Histogram-equalized image (note the washed-out appearance).  
(c) Histogram of (b).

a c  
b  
d

**FIGURE 3.22**

(a) Specified histogram.  
(b) Curve (1) is from Eq. (3.3-14), using the histogram in (a); curve (2) was obtained using the iterative procedure in Eq. (3.3-17).  
(c) Enhanced image using mappings from curve (2).  
(d) Histogram of (c).



- **Local Enhancement**

- define a square or rectangular neighborhood and move the center of this area from pixel to pixel.
- In [Fig. 3.23](#), a result of local processing using relatively small neighborhoods.

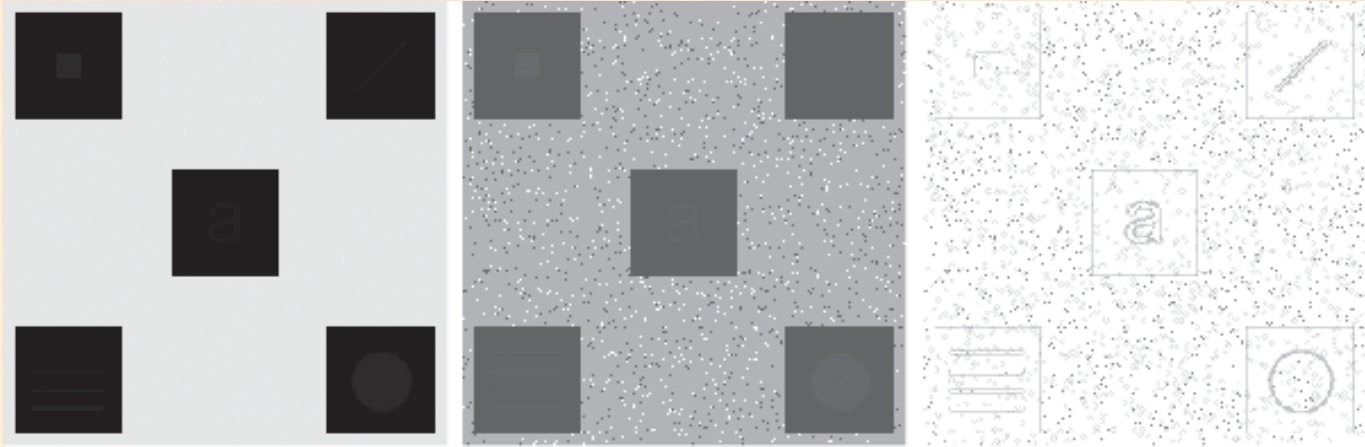
- Example 3.6 pp.105

- Eq. 3.3-21
- Eq. 3.3-22

a b c

**FIGURE 3.26**

(a) Original image. (b) Result of global histogram equalization. (c) Result of local histogram equalization.



a b

**FIGURE 3.27**

(a) Original image. (b) Result of local enhancement based on local histogram statistics. Compare (b) with Fig. 3.26(c).

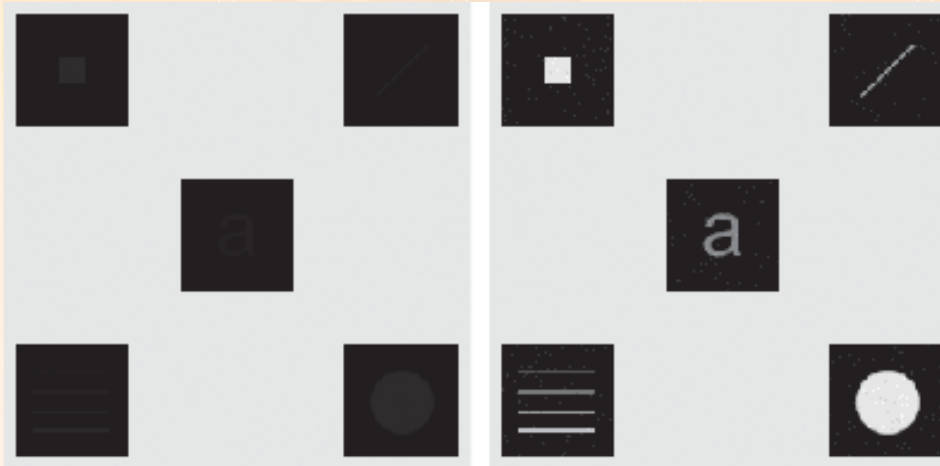
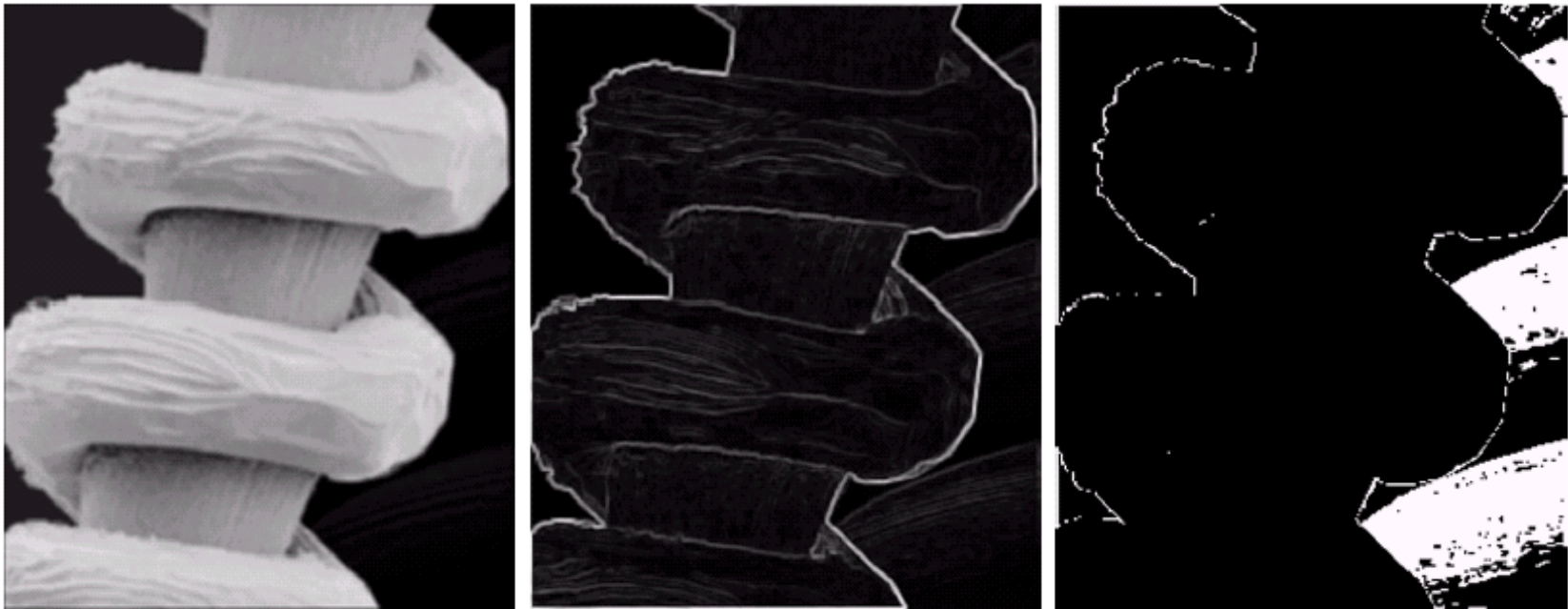




**FIGURE 3.24** SEM image of a tungsten filament and support, magnified approximately 130 $\times$ . (Original image courtesy of Mr. Michael Shaffer, Department of Geological Sciences, University of Oregon, Eugene).







a b c

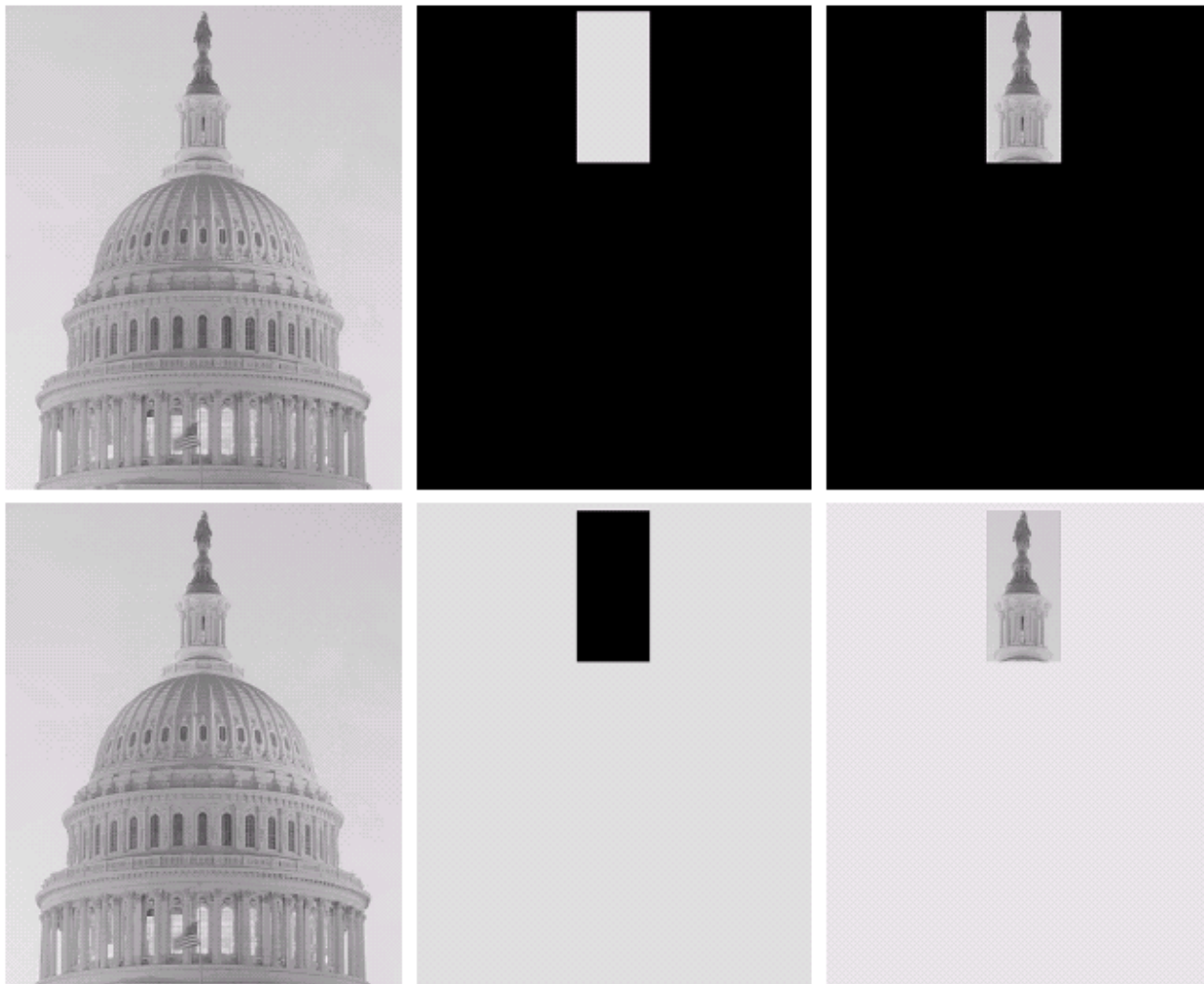
**FIGURE 3.25** (a) Image formed from all local means obtained from Fig. 3.24 using Eq. (3.3-21). (b) Image formed from all local standard deviations obtained from Fig. 3.24 using Eq. (3.3-22). (c) Image formed from all multiplication constants used to produce the enhanced image shown in Fig. 3.26.



**FIGURE 3.26**  
Enhanced SEM  
image. Compare  
with Fig. 3.24. Note  
in particular the  
enhanced area on  
the right side of  
the image.

## 3.4 Enhancement Using Arithmetic/Logic Operations

- Arithmetic/logic operations involving images are performed on a pixel-by-pixel basis between two or more images.
  - The AND and OR operations are used for *masking*; that is, for selecting subimages in an image, as illustrated in [Fig. 3.27](#).
  - Masking sometimes is referred to as *region of interest (ROI)* processing.
- **Image Subtraction**
  - The difference between two images  $f(x, y)$  and  $h(x, y)$ , expressed as
$$g(x, y) = f(x, y) - h(x, y)$$
  - [Figure 3.28](#)



a	b	c
d	e	f

**FIGURE 3.27**

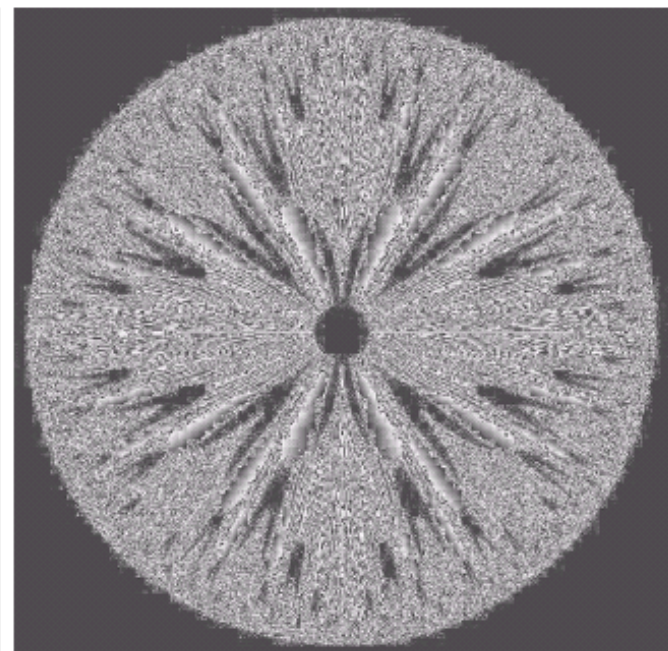
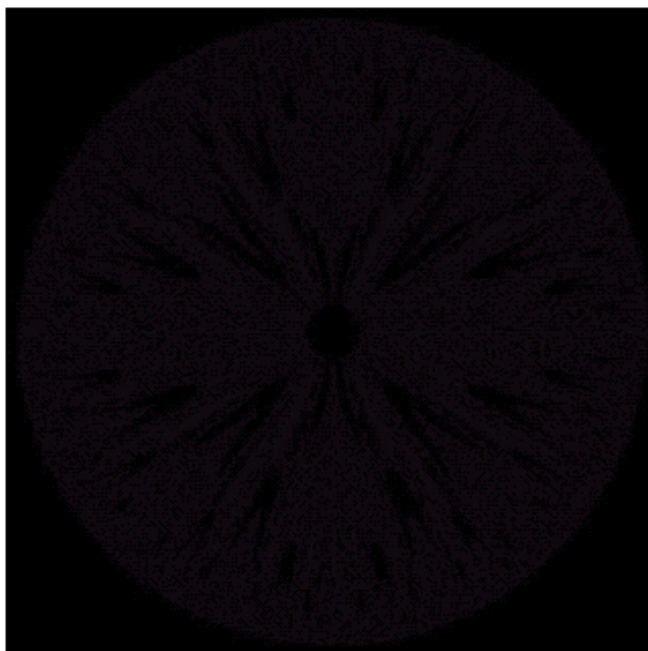
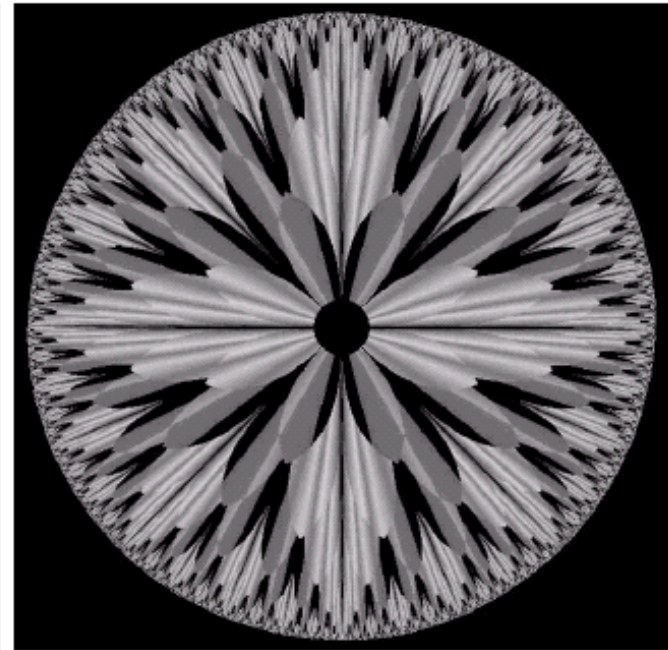
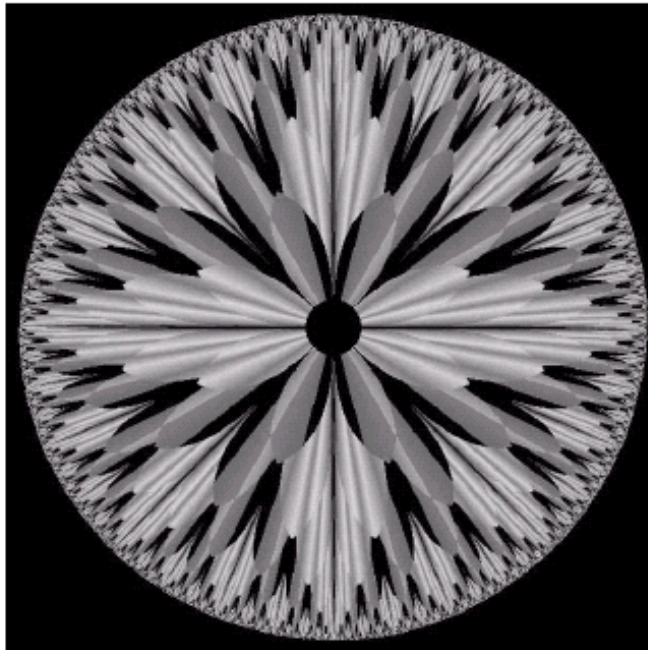
(a) Original image. (b) AND image mask. (c) Result of the AND operation on images (a) and (b). (d) Original image. (e) OR image mask. (f) Result of operation OR on images (d) and (e).



a b  
c d

**FIGURE 3.28**

(a) Original fractal image.  
(b) Result of setting the four lower-order bit planes to zero.  
(c) Difference between (a) and (b).  
(d) Histogram-equalized difference image. (Original image courtesy of Ms. Melissa D. Binde, Swarthmore College, Swarthmore, PA).



- **EXAMPLE 3.7**

- Use of image subtraction in *mask mode radiography*.

- **FIGURE 3.29**

- **Image Averaging**

- Consider a noisy image  $g(x, y)$  formed by the addition of noise  $\eta(x, y)$  to an original image  $f(x, y)$ ;

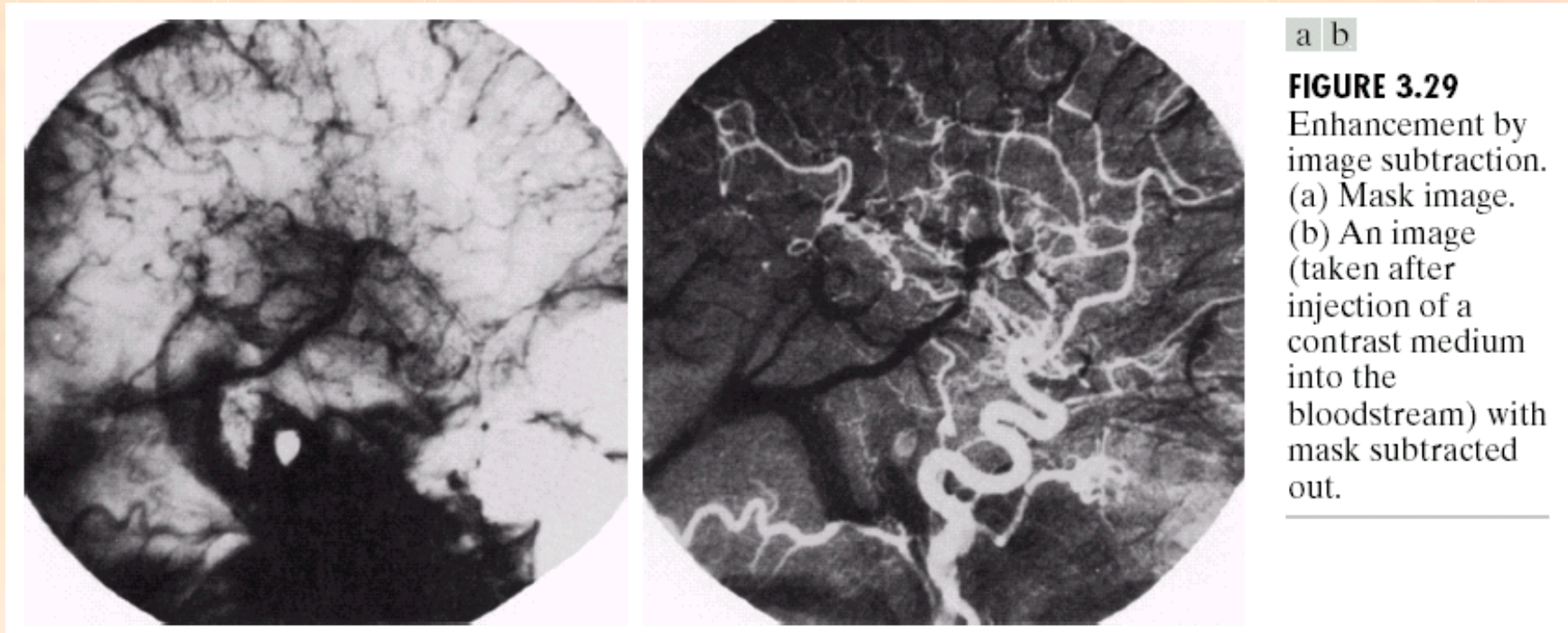
$$g(x, y) = f(x, y) + \eta(x, y)$$

- **EXAMPLE 3.8**

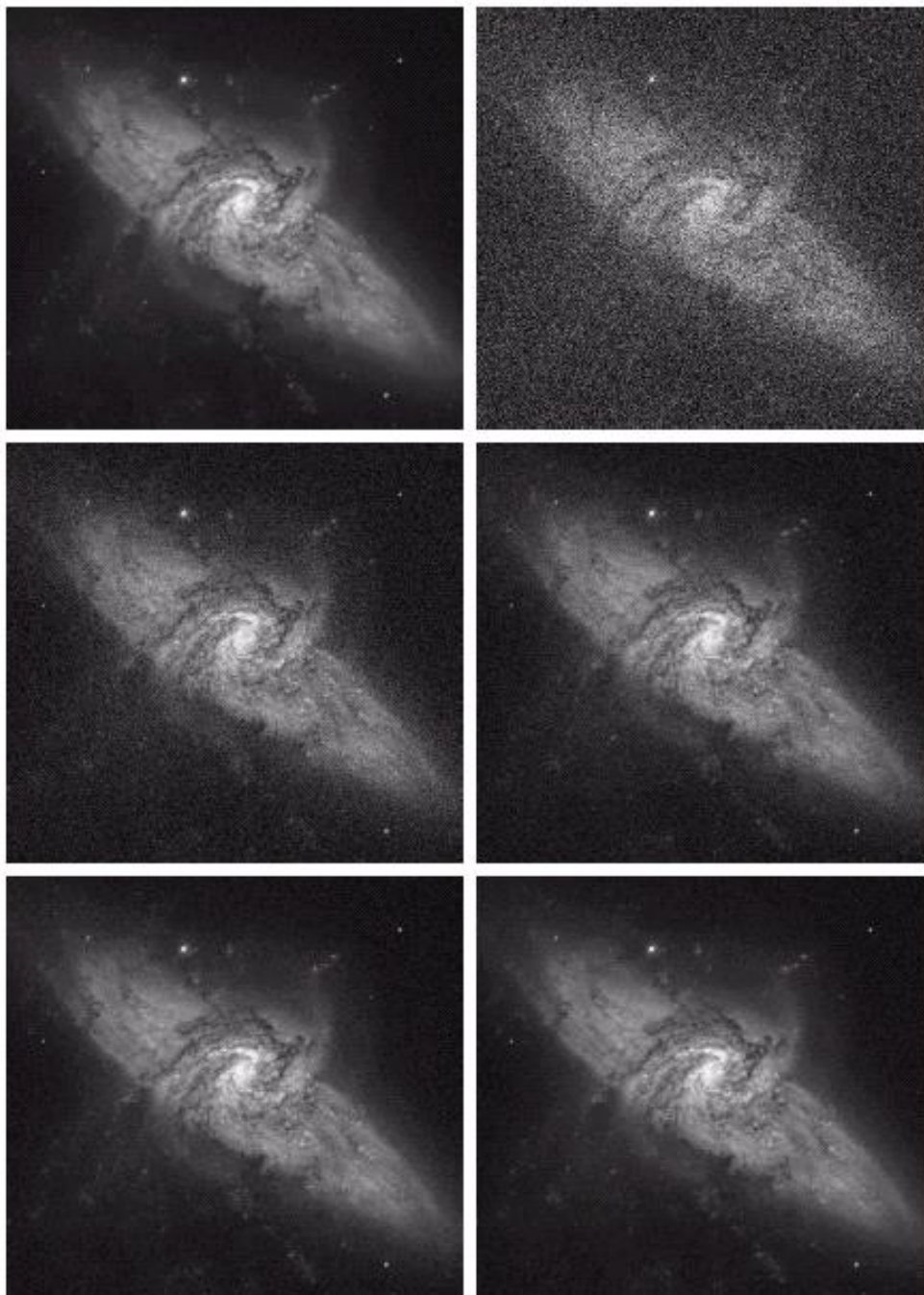
- Noise reduction by image averaging.

- **FIGURE 3.30 and FIGURE 3.31**





$$g(x, y) = f(x, y) - h(x, y)$$



$$g(x, y) = f(x, y) + \eta(x, y)$$

Averaging  $M$  noisy images

$$\bar{g}(x, y) = \frac{1}{M} \sum_{i=1}^M g_i(x, y)$$

It follows

$$E\{\bar{g}(x, y)\} = f(x, y)$$

and

$$\sigma_{\bar{g}(x, y)}^2 = \frac{1}{M} \sigma_{\eta(x, y)}^2$$

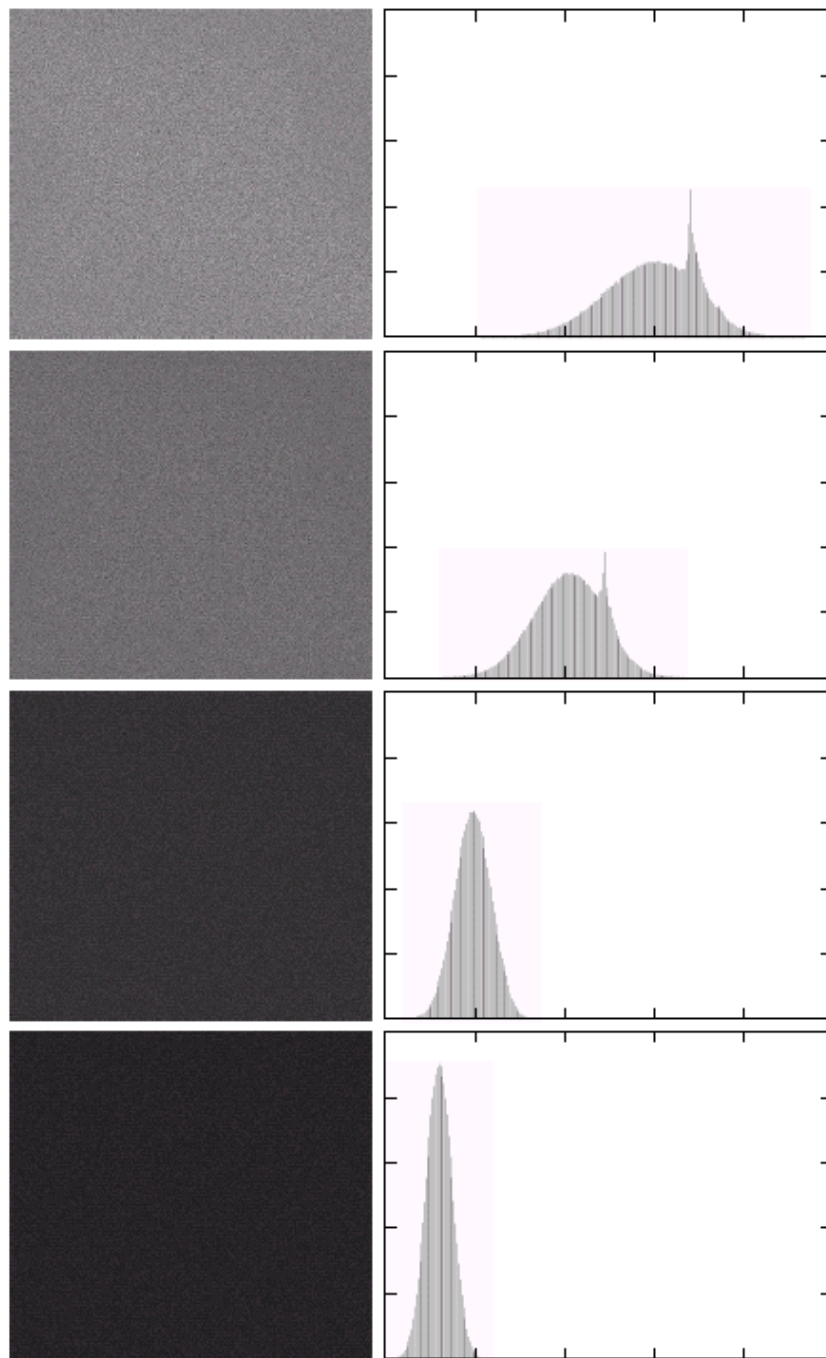
or

$$\sigma_{\bar{g}(x, y)} = \frac{1}{\sqrt{M}} \sigma_{\eta(x, y)}$$

a b  
c d  
e f

**FIGURE 3.30** (a) Image of Galaxy Pair NGC 3314. (b) Image corrupted by additive Gaussian noise with zero mean and a standard deviation of 64 gray levels. (c)–(f) Results of averaging  $K = 8, 16, 64$ , and  $128$  noisy images. (Original image courtesy of NASA.)





a b

**FIGURE 3.31**

(a) From top to bottom: Difference images between Fig. 3.30(a) and the four images in Figs. 3.30(c) through (f), respectively. (b) Corresponding histograms.

# 3.5 Basics of Spatial Filtering

- Some neighborhood operations work with the values of the image pixels in the neighborhood *and* the corresponding values of a subimage that has the same dimensions as the neighborhood.
- The subimage is called a *filter*, *mask*, *kernel*, *template*, or *window*.
- The values in a filter subimage are referred to as *coefficients*, rather than pixels.
  - The mechanics of spatial filtering are illustrated in [Fig. 3.32](#).

**FIGURE 3.28**

The mechanics of linear spatial filtering using a  $3 \times 3$  kernel. The pixels are shown as squares to simplify the graphics. Note that the origin of the image is at the top left, but the origin of the kernel is at its center. Placing the origin at the center of spatially symmetric kernels simplifies writing expressions for linear filtering.

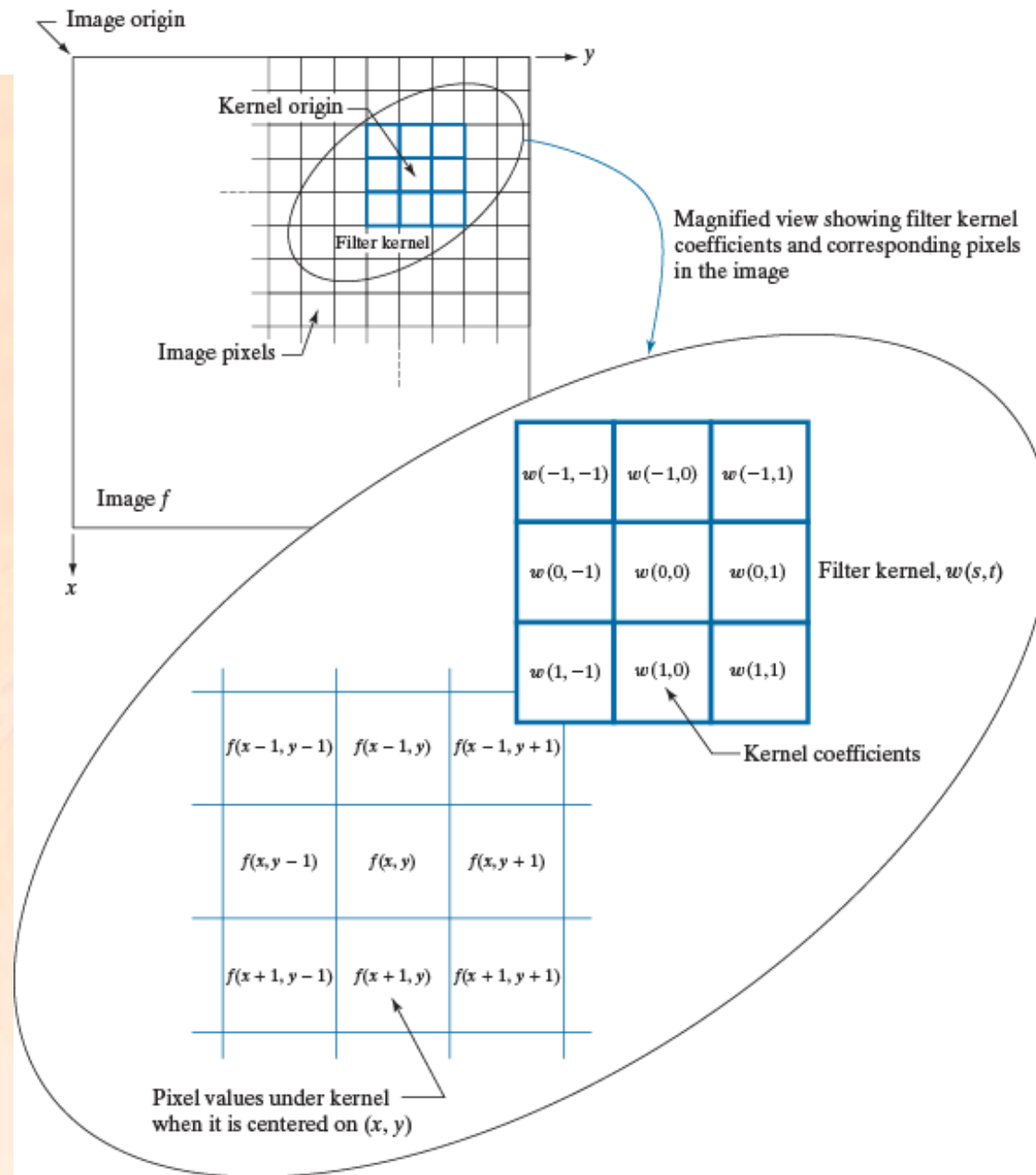


**FIGURE 3.29**

Illustration of 1-D correlation and convolution of a kernel,  $w$ , with a function  $f$  consisting of a discrete unit impulse. Note that correlation and convolution are functions of the variable  $x$ , which acts to *displace* one function with respect to the other. For the extended correlation and convolution results, the starting configuration places the right-most element of the kernel to be coincident with the origin of  $f$ . Additional padding must be used.

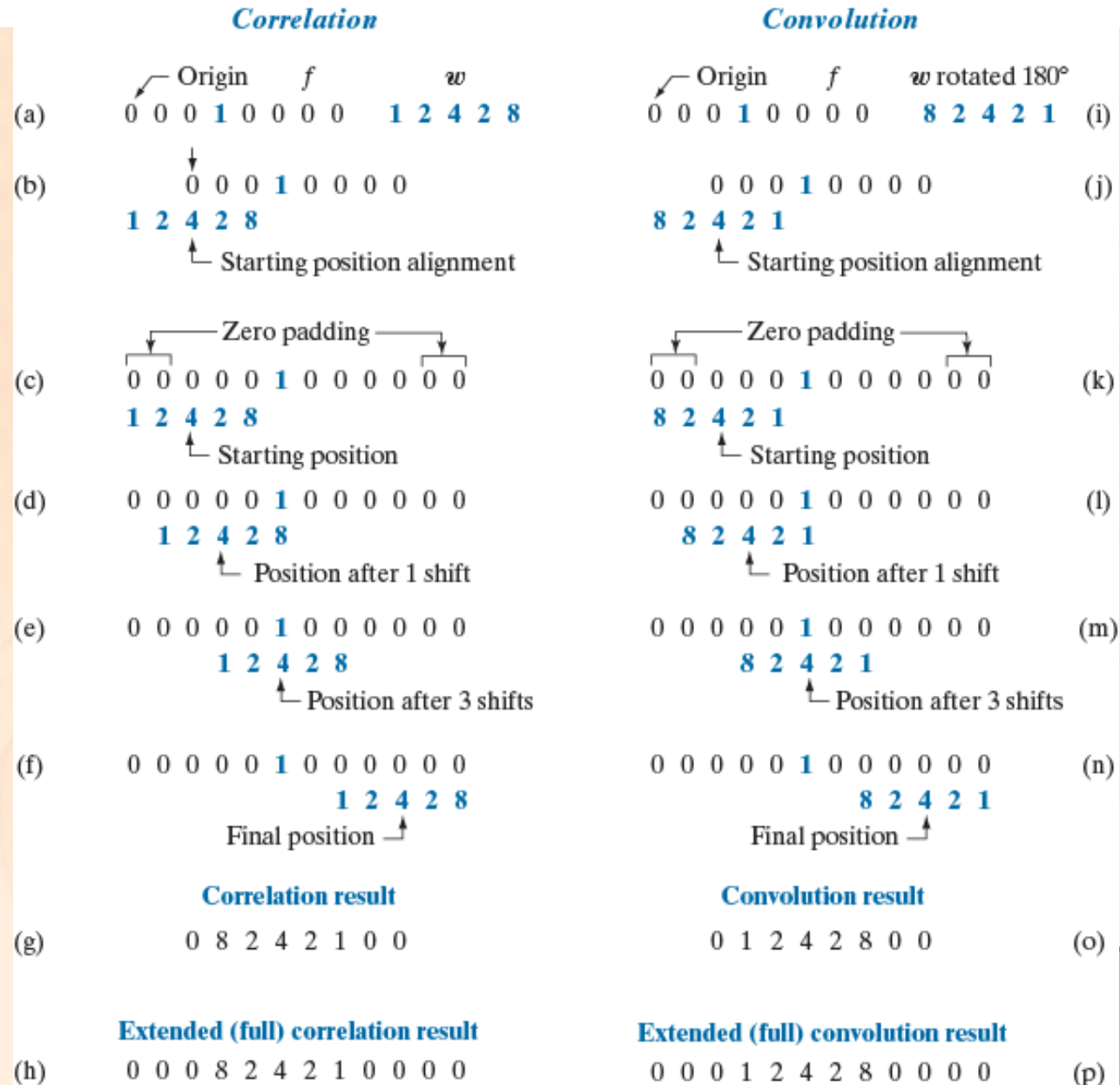
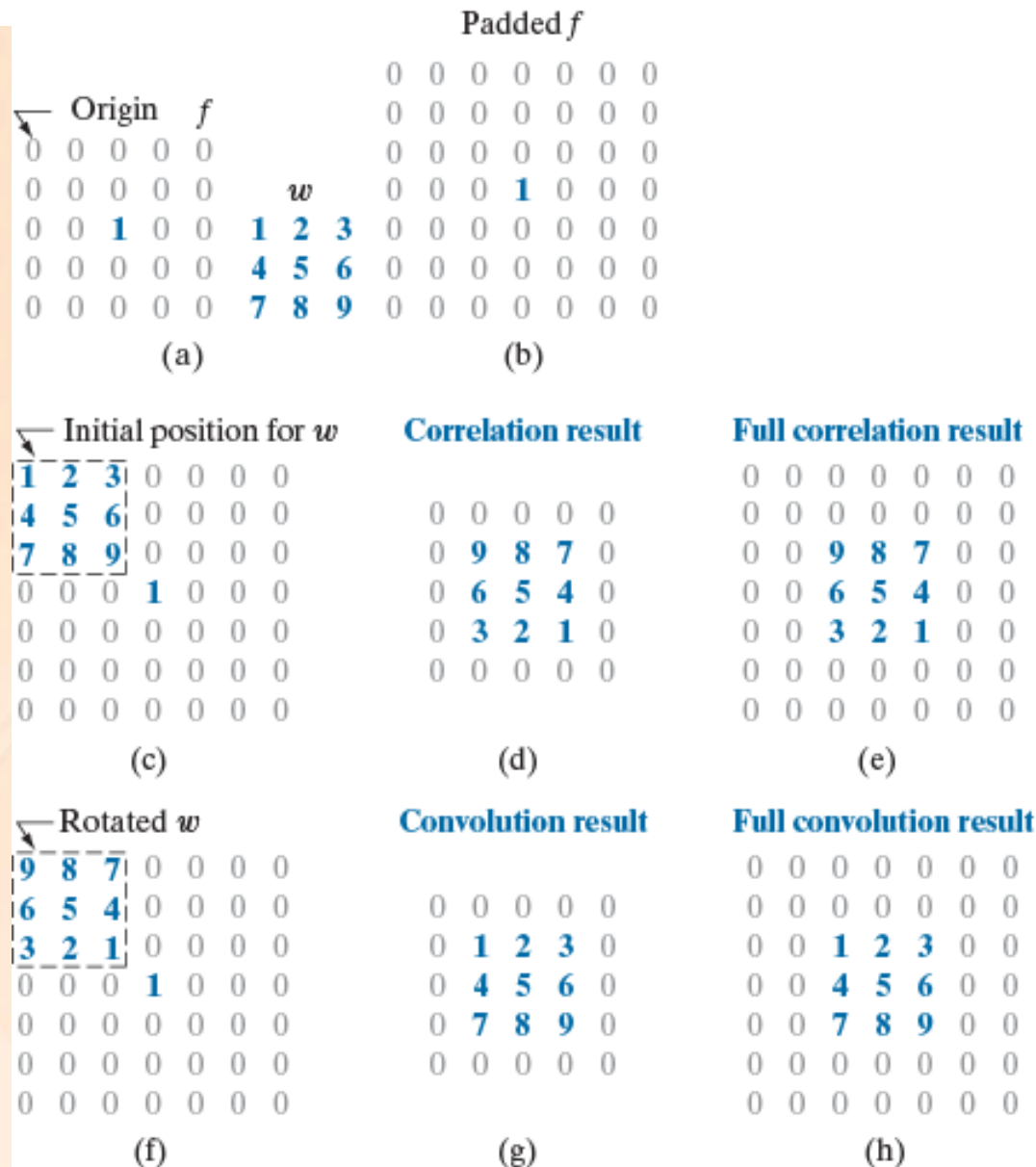




**FIGURE 3.30**

Correlation (middle row) and convolution (last row) of a 2-D kernel with an image consisting of a discrete unit impulse. The 0's are shown in gray to simplify visual analysis. Note that correlation and convolution are functions of  $x$  and  $y$ . As these variable change, they *displace* one function with respect to the other. See the discussion of Eqs. (3-36) and (3-37) regarding full correlation and convolution.



- For the  $3 \times 3$  mask, the result (or response),  $R$ , of linear filtering with the filter mask at a point  $(x, y)$  in the image is

$$R = w(-1, -1)f(x - 1, y - 1) + w(-1, 0)f(x - 1, y) + \dots + w(0, 0)f(x, y) + p + w(1, 0)f(x + 1, y) + w(1, 1)f(x + 1, y + 1)$$

- For a mask of size  $m \times n$  (on masks of *odd* sizes)
  - assume that  $m=2a+1$  and  $n=2b+1$
  - where  $a$  and  $b$  are nonnegative integers.

- linear filtering of an image  $f$  of size  $M \times N$ 
  - with a filter mask of size  $m \times n$  is given by the expression:

$$g(x, y) = \sum_{s=-a}^a \sum_{t=-b}^b w(s, t) f(x + s, y + t) \quad (3.5-1)$$

$$a=(m-1)/2 \text{ and } b=(n-1)/2$$

- For the  $3 \times 3$  general mask shown in [Fig. 3.33](#) the response at any point  $(x, y)$  in the image is given by

$$\begin{aligned} R &= w_1 z_1 + w_2 z_2 + \dots w_9 z_9 \\ &= \sum_{i=1}^9 w_i z_i. \end{aligned} \quad (3.5-3)$$

**FIGURE 3.33**

Another  
representation of  
a general  $3 \times 3$   
spatial filter mask.

---

$w_1$	$w_2$	$w_3$
$w_4$	$w_5$	$w_6$
$w_7$	$w_8$	$w_9$



- **Smoothing Linear Filters**

- *Averaging filters* – average of the pixels contained in the neighborhood of the filter mask.

$$R = \frac{1}{9} \sum_{i=1}^9 z_i,$$

- Eq. 3.6-1
  - Figure 3.34 shows two  $3 \times 3$  smoothing filters.

$$\frac{1}{9} \times \begin{array}{|c|c|c|} \hline 1 & 1 & 1 \\ \hline 1 & 1 & 1 \\ \hline 1 & 1 & 1 \\ \hline \end{array} \quad \frac{1}{16} \times \begin{array}{|c|c|c|} \hline 1 & 2 & 1 \\ \hline 2 & 4 & 2 \\ \hline 1 & 2 & 1 \\ \hline \end{array}$$

a b

**FIGURE 3.34** Two  $3 \times 3$  smoothing (averaging) filter masks. The constant multiplier in front of each mask is equal to the sum of the values of its coefficients, as is required to compute an average.

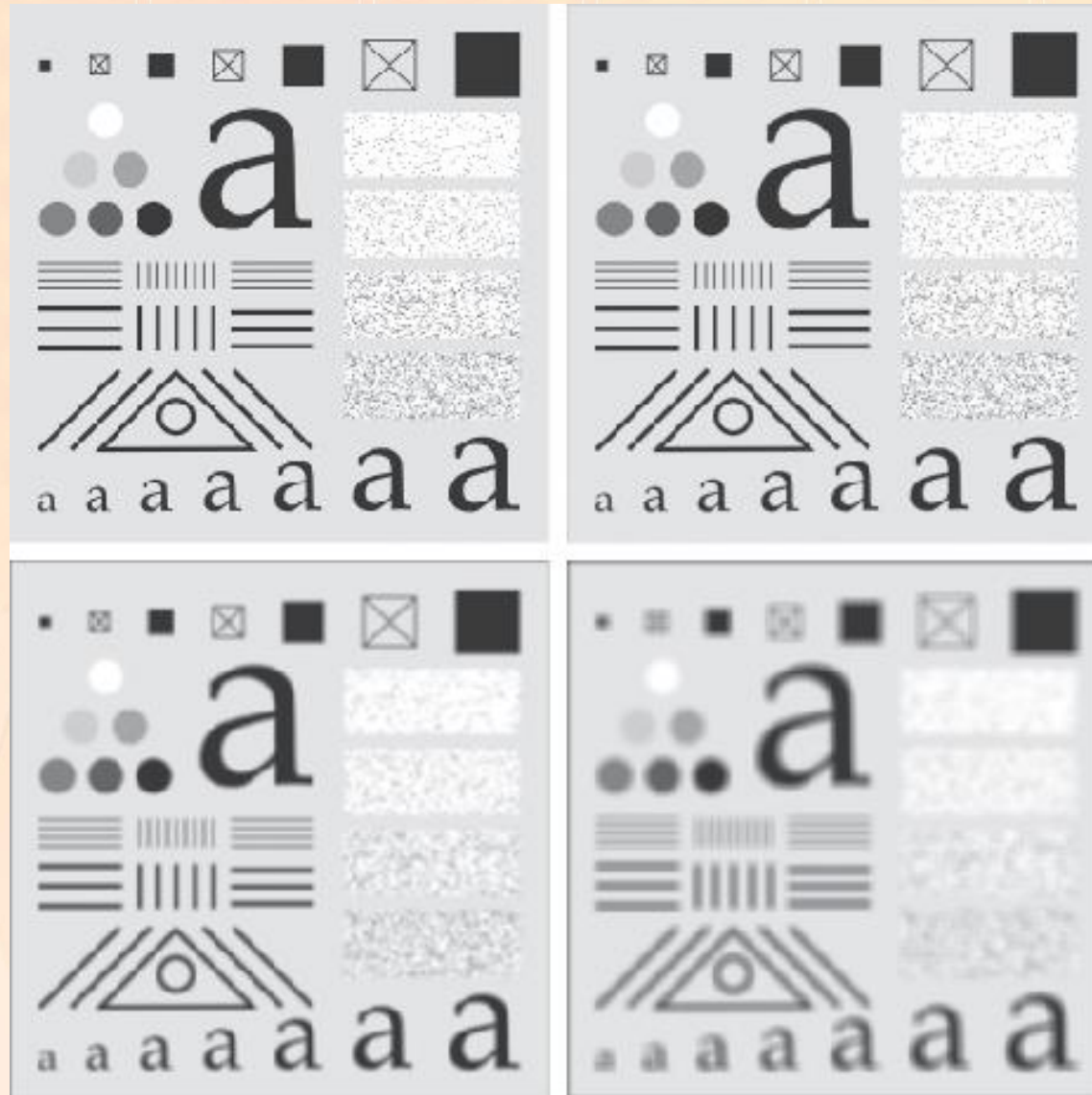
- **EXAMPLE 3.9**

- Image smoothing with masks of various sizes.
- The effects of smoothing as a function of filter size are illustrated in [Fig. 3.35](#).
- As mentioned earlier, an important application of spatial averaging is to blur an image for the purpose getting a gross representation of objects of interest.
  - [Figure 3.36](#)

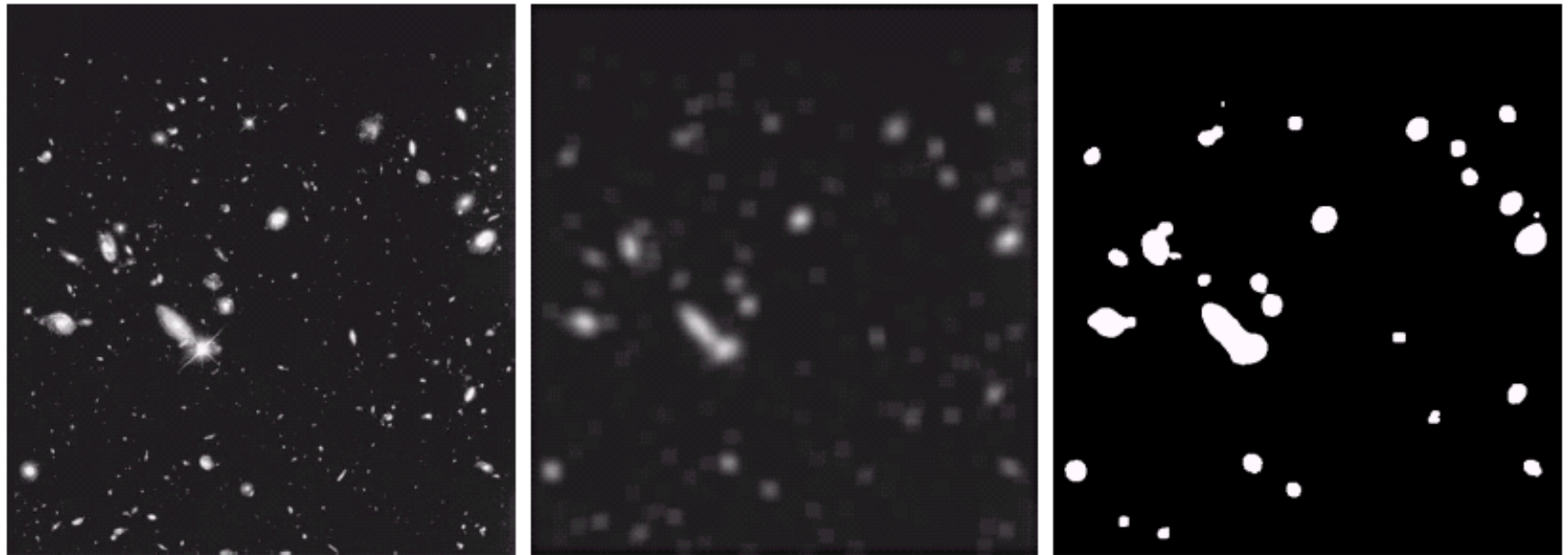
a	b
c	d

**FIGURE 3.33**

(a) Test pattern of size  $1024 \times 1024$  pixels.  
(b)-(d) Results of lowpass filtering with box kernels of sizes  $3 \times 3$ ,  $11 \times 11$ , and  $21 \times 21$ , respectively.





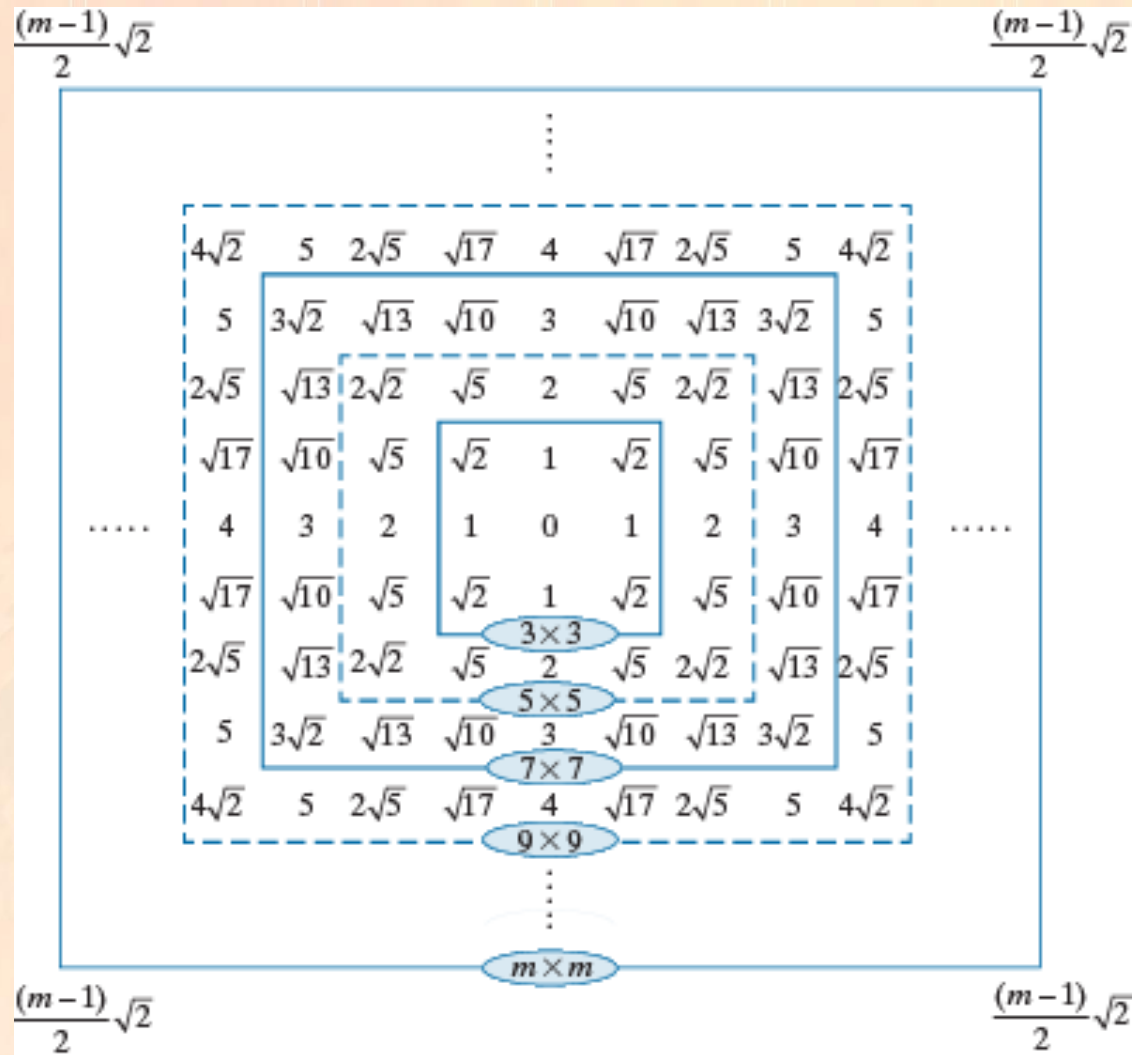


a b c

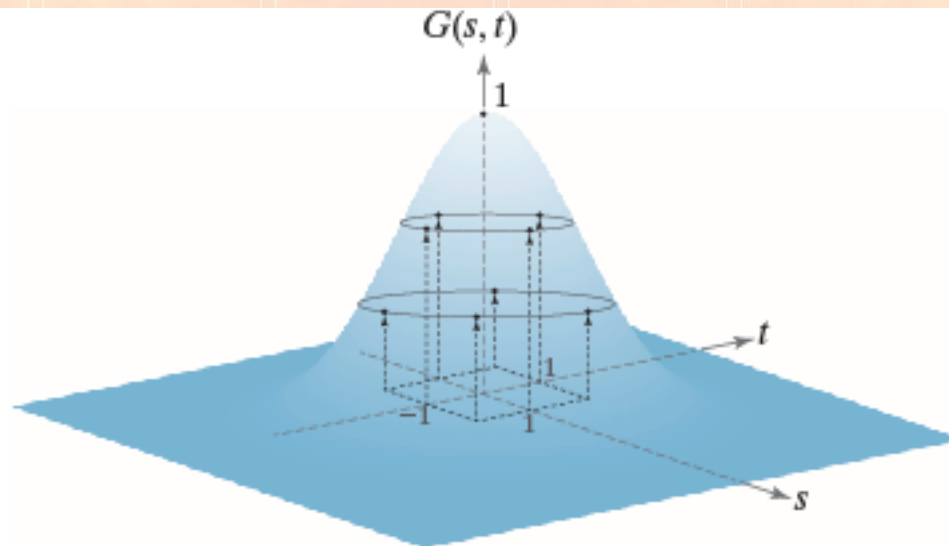
**FIGURE 3.36** (a) Image from the Hubble Space Telescope. (b) Image processed by a  $15 \times 15$  averaging mask. (c) Result of thresholding (b). (Original image courtesy of NASA.)

**FIGURE 3.34**

Distances from the center for various sizes of square kernels.



**a b**  
**FIGURE 3.35**  
(a) Sampling a Gaussian function to obtain a discrete Gaussian kernel. The values shown are for  $K = 1$  and  $\sigma = 1$ . (b) Resulting  $3 \times 3$  kernel [this is the same as Fig. 3.31(b)].



$$\frac{1}{4.8976} \times$$

0.3679	0.6065	0.3679
0.6065	1.0000	0.6065
0.3679	0.6065	0.3679



a b c

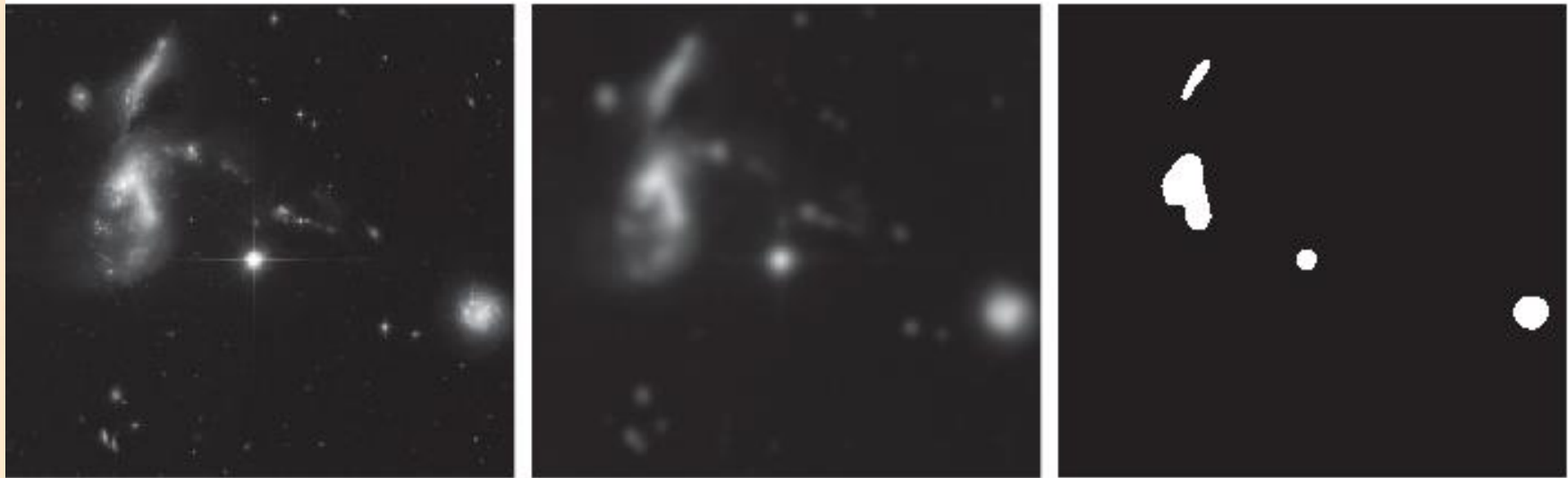
**FIGURE 3.36** (a) A test pattern of size  $1024 \times 1024$ . (b) Result of lowpass filtering the pattern with a Gaussian kernel of size  $21 \times 21$ , with standard deviations  $\sigma = 3.5$ . (c) Result of using a kernel of size  $43 \times 43$ , with  $\sigma = 7$ . This result is comparable to Fig. 3.33(d). We used  $K = 1$  in all cases.



a b c

**FIGURE 3.37** (a) Result of filtering Fig. 3.36(a) using a Gaussian kernels of size  $43 \times 43$ , with  $\sigma = 7$ . (b) Result of using a kernel of  $85 \times 85$ , with the same value of  $\sigma$ . (c) Difference image.





a b c

**FIGURE 3.41** (a) A  $2566 \times 2758$  Hubble Telescope image of the *Hickson Compact Group*. (b) Result of lowpass filtering with a Gaussian kernel. (c) Result of thresholding the filtered image (intensities were scaled to the range  $[0, 1]$ ). The Hickson Compact Group contains dwarf galaxies that have come together, setting off thousands of new star clusters. (Original image courtesy of NASA.)

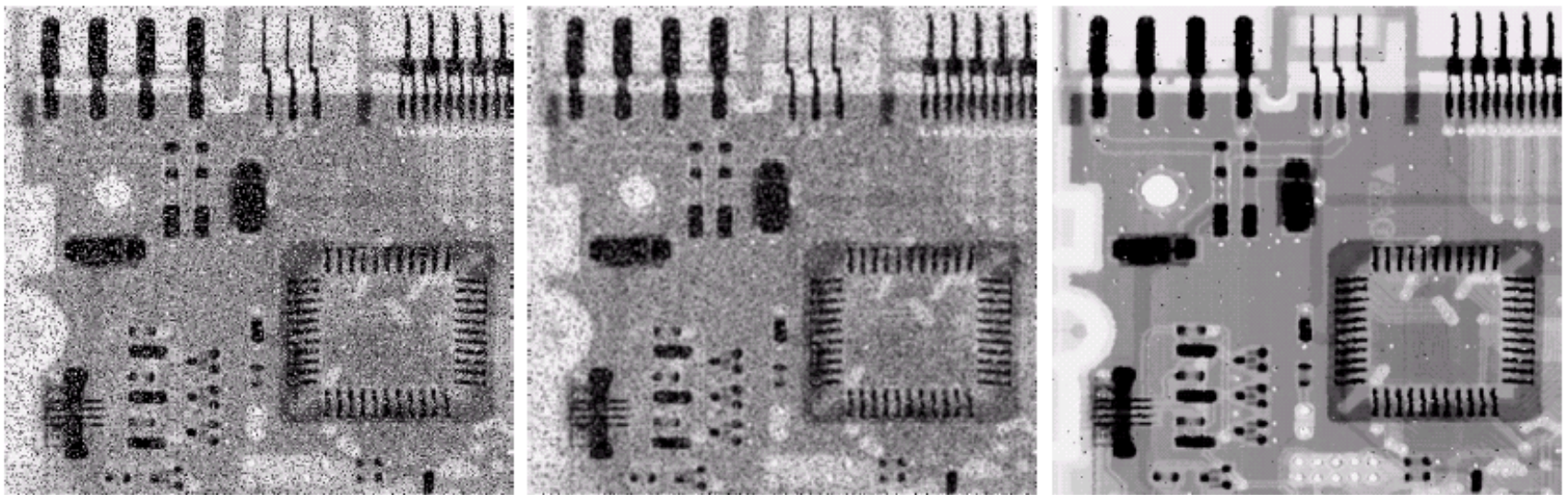
- **Order-Statistics Filters**

- *median filter*

- Median filters are particularly effective in the presence of *impulse noise*, also called *salt-and-pepper noise*.

- **EXAMPLE 3.10**

- Use of median filtering for noise reduction.
  - Figure 3.37



a b c

**FIGURE 3.37** (a) X-ray image of circuit board corrupted by salt-and-pepper noise. (b) Noise reduction with a  $3 \times 3$  averaging mask. (c) Noise reduction with a  $3 \times 3$  median filter. (Original image courtesy of Mr. Joseph E. Pascente, Lixi, Inc.)

- Some detail sharpening filters that are based on first- and second-order derivatives, respectively.
  - The derivatives of a digital function are defined in terms of differences.

$$\frac{\partial f}{\partial x} = f(x+1) - f(x)$$

$$\frac{\partial^2 f}{\partial^2 x} = f(x+1) + f(x-1) - 2f(x)$$

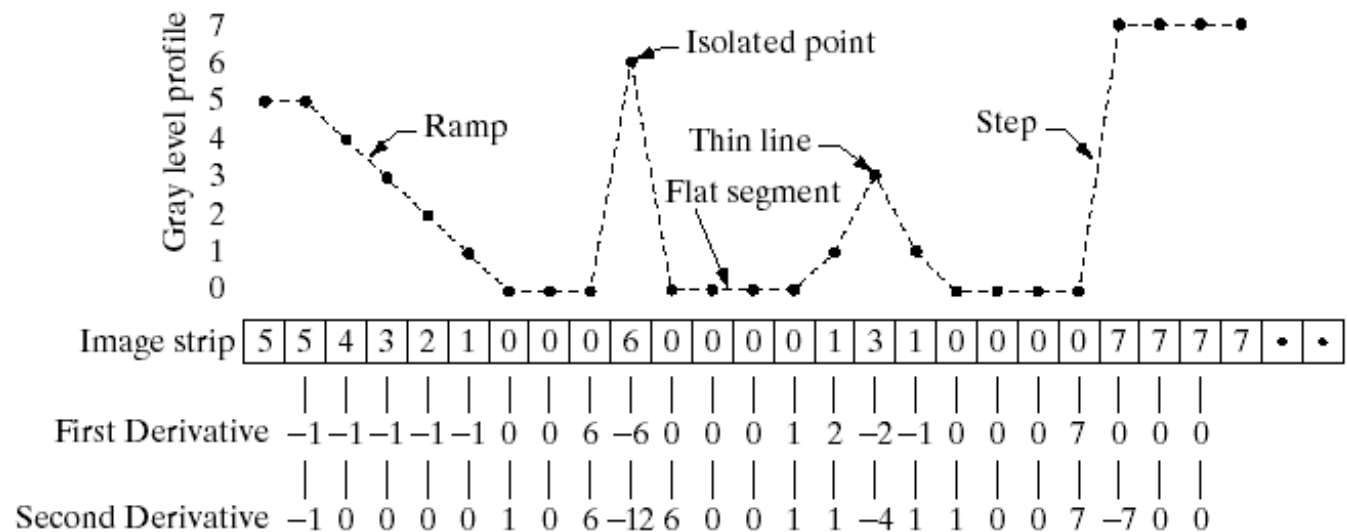
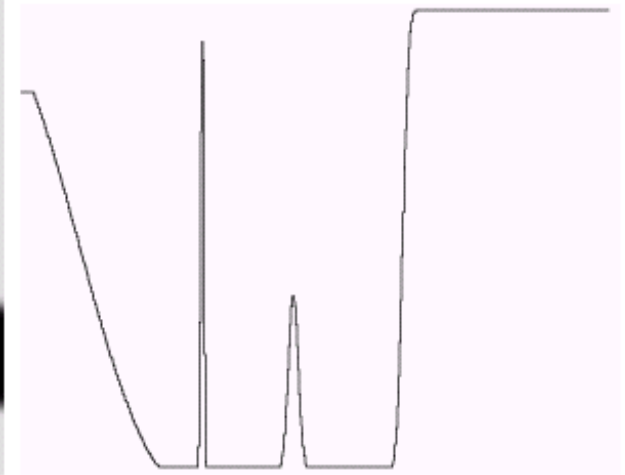
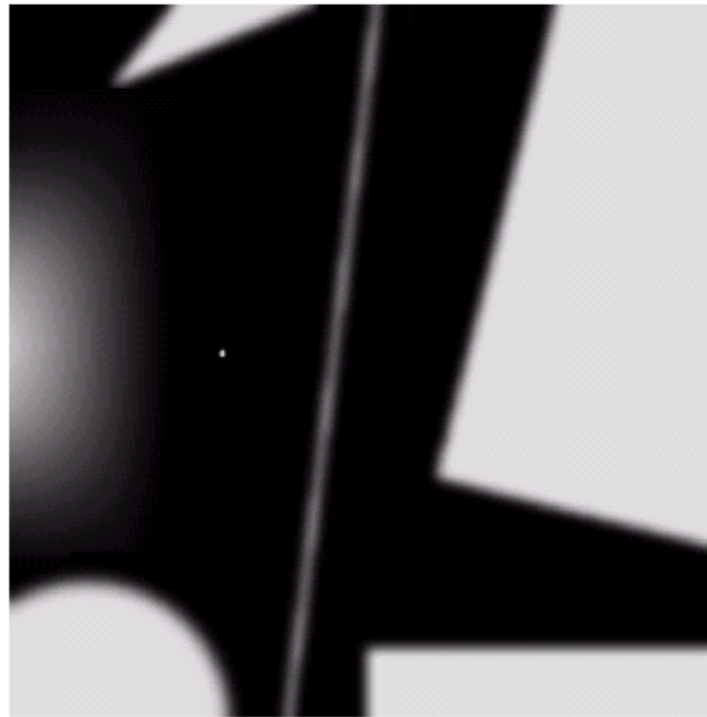
- fundamental similarities and differences between first- and second-order derivatives, shown in [Fig. 3.38](#).



a b  
c

**FIGURE 3.38**

(a) A simple image. (b) 1-D horizontal gray-level profile along the center of the image and including the isolated noise point. (c) Simplified profile (the points are joined by dashed lines to simplify interpretation).

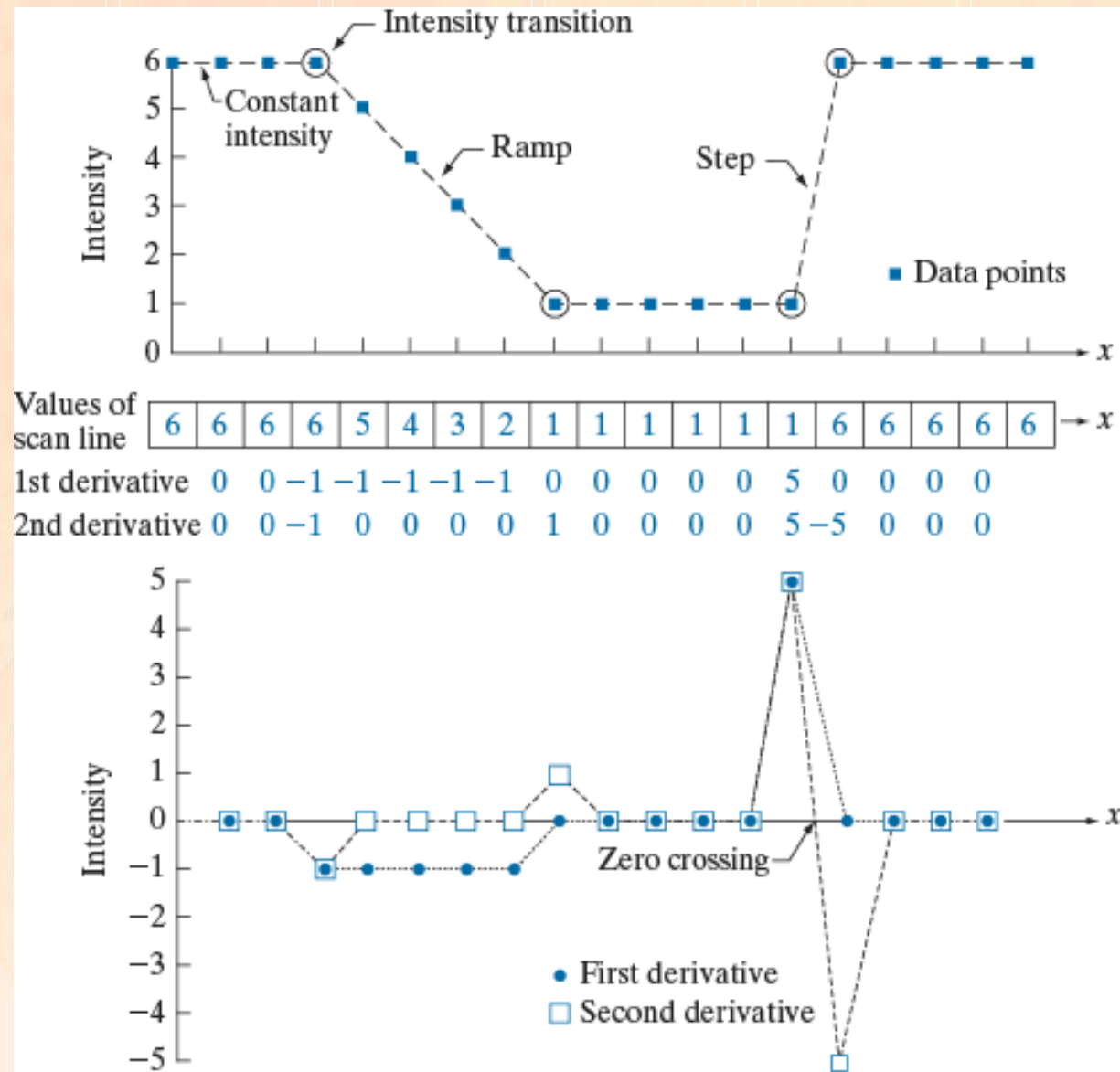


a  
b  
c**FIGURE 3.44**

(a) A section of a horizontal scan line from an image, showing ramp and step edges, as well as constant segments.

(b) Values of the scan line and its derivatives.

(c) Plot of the derivatives, showing a zero crossing. In (a) and (c) points were joined by dashed lines as a visual aid.



- Comparison between first- and second-order derivatives,
  - First-order derivatives generally produce **thicker edges** in an image.
  - Second-order derivatives have a stronger response to **fine detail**, such as thin lines and isolated points.
  - First-order derivatives generally have a stronger response to a **gray-level step**.
  - Second-order derivatives produce a double response at **step changes in gray level**.
- We also note of second-order derivatives that, for similar changes in gray-level values in an image, their response is stronger to a line than to a step, and to a point than to a line.

- **Laplacian**
  - **use of Second Derivatives for Enhancement**

$$\nabla^2 f = \frac{\partial^2 f}{\partial x^2} + \frac{\partial^2 f}{\partial y^2}. \quad (3.7-1)$$

- using the mask shown in Fig. [3.39](#).
- Eq. 3.7-5
- **EXAMPLE 3.11**
  - [Figure 3.40](#)



0	1	0	1	1	1
1	-4	1	1	-8	1
0	1	0	1	1	1

0	-1	0	-1	-1	-1
-1	4	-1	-1	8	-1
0	-1	0	-1	-1	-1

a	b
c	d

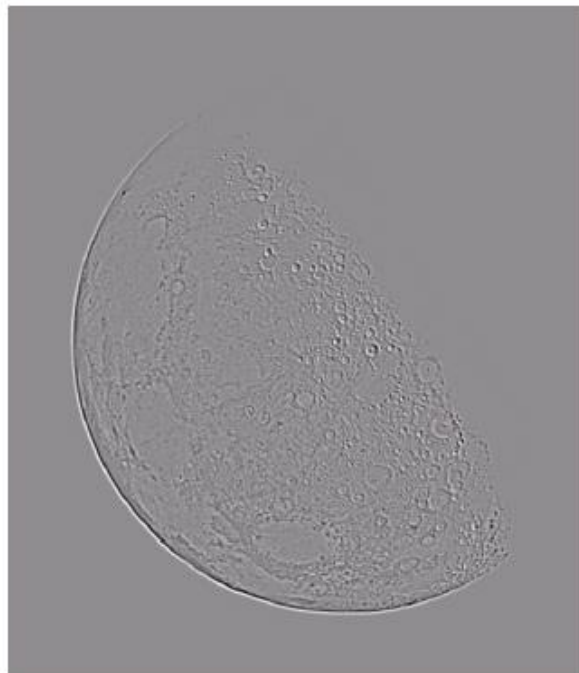
**FIGURE 3.39**

(a) Filter mask used to implement the digital Laplacian, as defined in Eq. (3.7-4).  
(b) Mask used to implement an extension of this equation that includes the diagonal neighbors. (c) and (d) Two other implementations of the Laplacian.

a b  
c d

**FIGURE 3.40**

(a) Image of the North Pole of the moon.  
(b) Laplacian-filtered image.  
(c) Laplacian image scaled for display purposes.  
(d) Image enhanced by using Eq. (3.7-5).  
(Original image courtesy of NASA.)



- Composite Laplacian mask

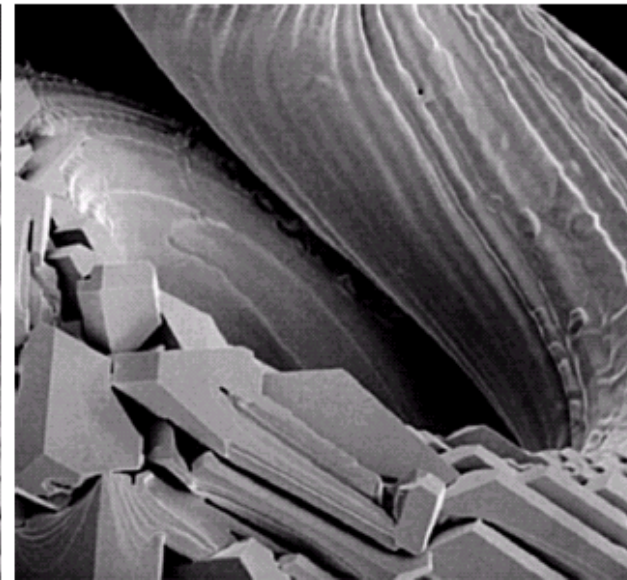
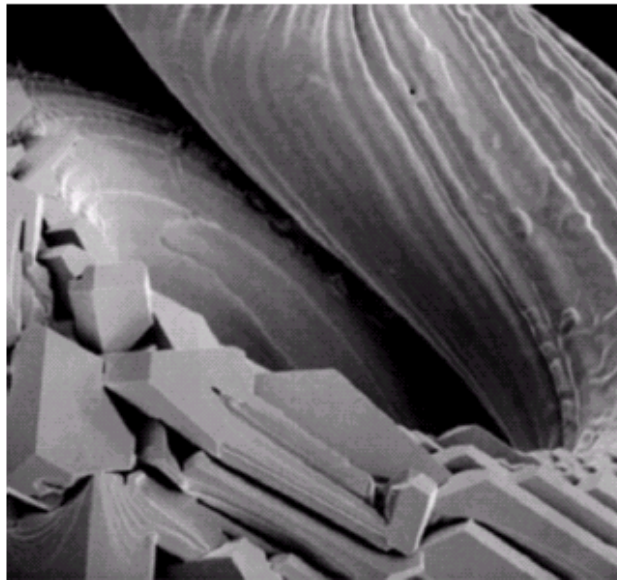
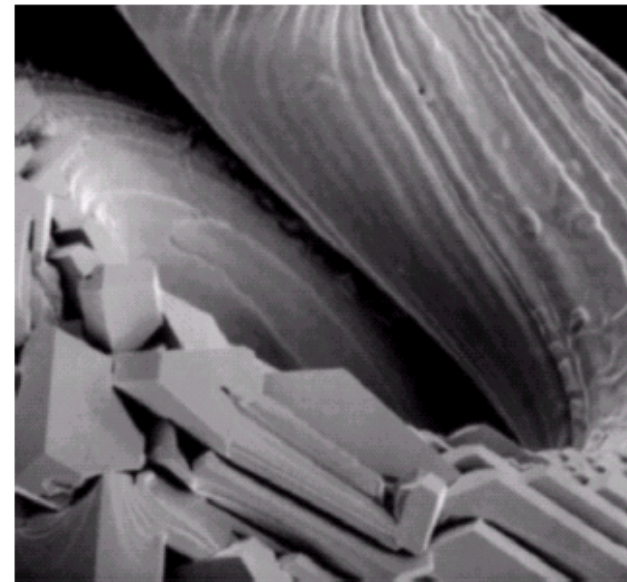
$$\begin{aligned} g(x, y) &= f(x, y) - [f(x + 1, y) + f(x - 1, y) \\ &\quad + f(x, y + 1) + f(x, y - 1)] + 4f(x, y) \\ &= 5f(x, y) - [f(x + 1, y) + f(x - 1, y) \\ &\quad + f(x, y + 1) + f(x, y - 1)]. \end{aligned} \quad (3.7-6)$$

- **EXAMPLE 3.12**

- Fig. 3.41

0	-1	0
-1	5	-1
0	-1	0

-1	-1	-1
-1	9	-1
-1	-1	-1



a b c  
d e

**FIGURE 3.41** (a) Composite Laplacian mask. (b) A second composite mask. (c) Scanning electron microscope image. (d) and (e) Results of filtering with the masks in (a) and (b), respectively. Note how much sharper (e) is than (d). (Original image courtesy of Mr. Michael Shaffer, Department of Geological Sciences, University of Oregon, Eugene.)



- **Unsharp masking and high-boost filtering**

- *unsharp masking*

$$f_s(x, y) = f(x, y) - \bar{f}(x, y) \quad (3.7-7)$$

- *high-boost filtering*

$$f_{hb}(x, y) = Af(x, y) - \bar{f}(x, y) \quad (3.7-8)$$

- Fig. 3.42
- **EXAMPLE 3.13**
  - Figure 3.43 shows such an application

0	-1	0	-1	-1	-1
-1	$A + 4$	-1	-1	$A + 8$	-1
0	-1	0	-1	-1	-1

a b

**FIGURE 3.42** The high-boost filtering technique can be implemented with either one of these masks, with  $A \geq 1$ .

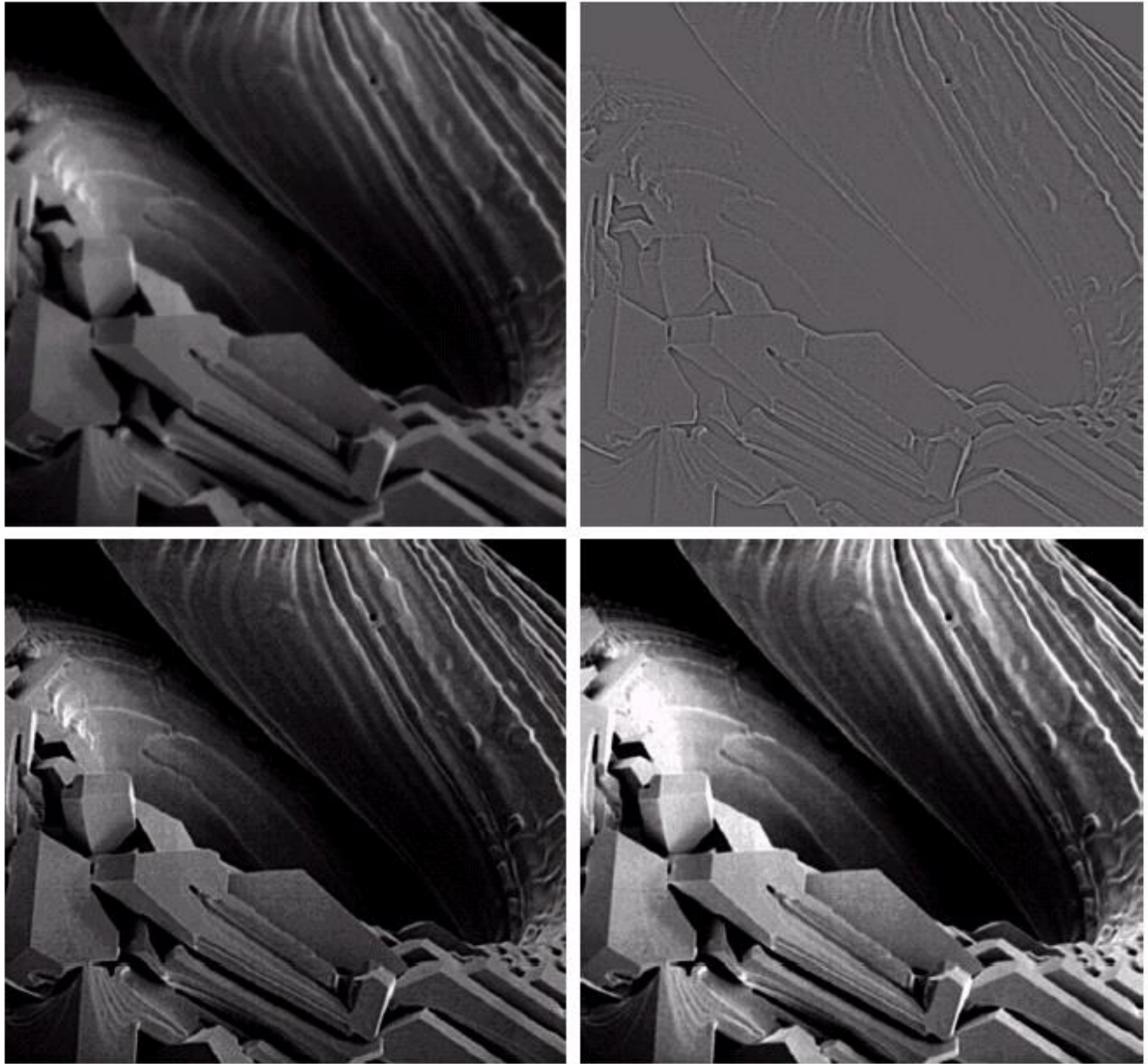
a b  
c d

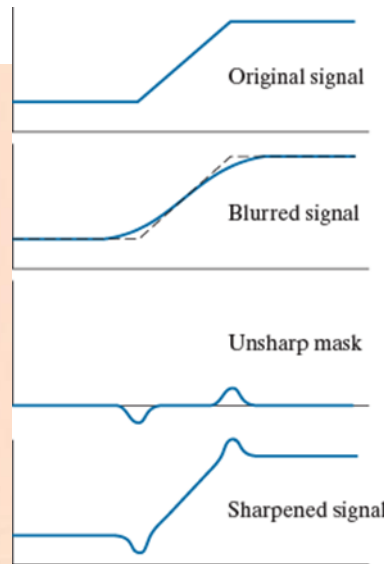
**FIGURE 3.43**

(a) Same as Fig. 3.41(c), but darker.

(b) Laplacian of (a) computed with the mask in Fig. 3.42(b) using  $A = 0$ .

(c) Laplacian enhanced image using the mask in Fig. 3.42(b) with  $A = 1$ . (d) Same as (c), but using  $A = 1.7$ .





a b c  
d e

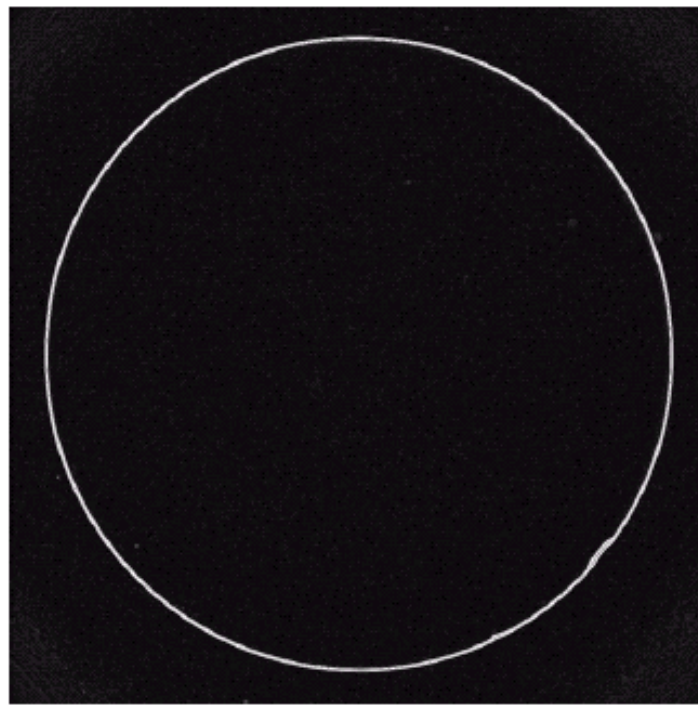
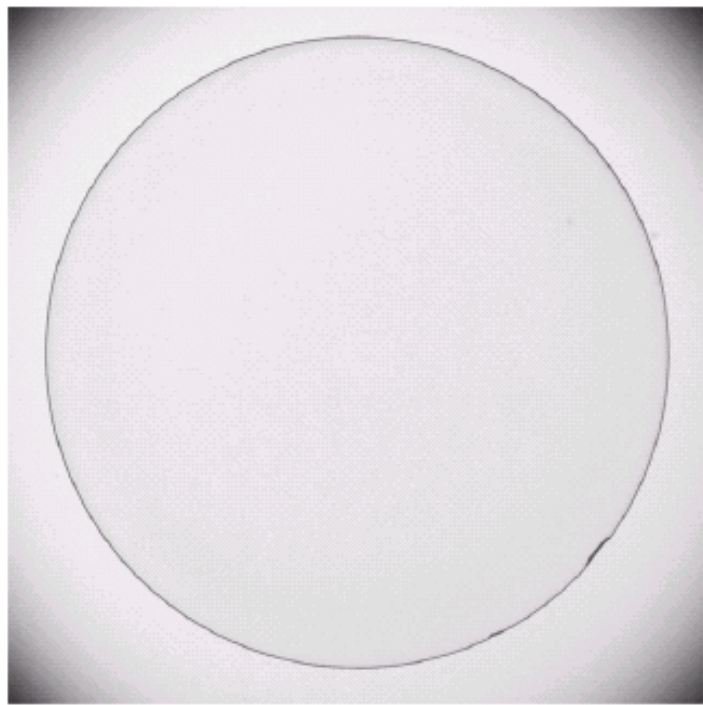
**FIGURE 3.49** (a) Original image of size  $600 \times 259$  pixels. (b) Image blurred using a  $31 \times 31$  Gaussian lowpass filter with  $\sigma = 5$ . (c) Mask. (d) Result of unsharp masking using Eq. (3-56) with  $k = 1$ . (e) Result of highboost filtering with  $k = 4.5$ .



- **Gradient**
  - **Use of First Derivatives for Enhancement**
    - **Eq. 3.7-12 & eq. 3.7-13**
    - use the notation in [Fig. 3.44.](#)
    - **EXAMPLE 3.14 – [Fig. 3.45.](#)**

A  $3 \times 3$  region of an image (the  $z$ 's are gray-level values) and masks used to compute the gradient at point labeled  $z_5$ . All masks coefficients sum to zero, as expected of a derivative operator.

-1	-2	-1	-1	0	1
0	0	0	-2	0	2
1	2	1	-1	0	1



a b

**FIGURE 3.45**  
Optical image of  
contact lens (note  
defects on the  
boundary at 4 and  
5 o'clock).  
(b) Sobel  
gradient.  
(Original image  
courtesy of  
Mr. Pete Sites,  
Perceptics  
Corporation.)

a b  
c d**FIGURE 3.52**

Transfer functions of ideal 1-D filters in the frequency domain ( $u$  denotes frequency).

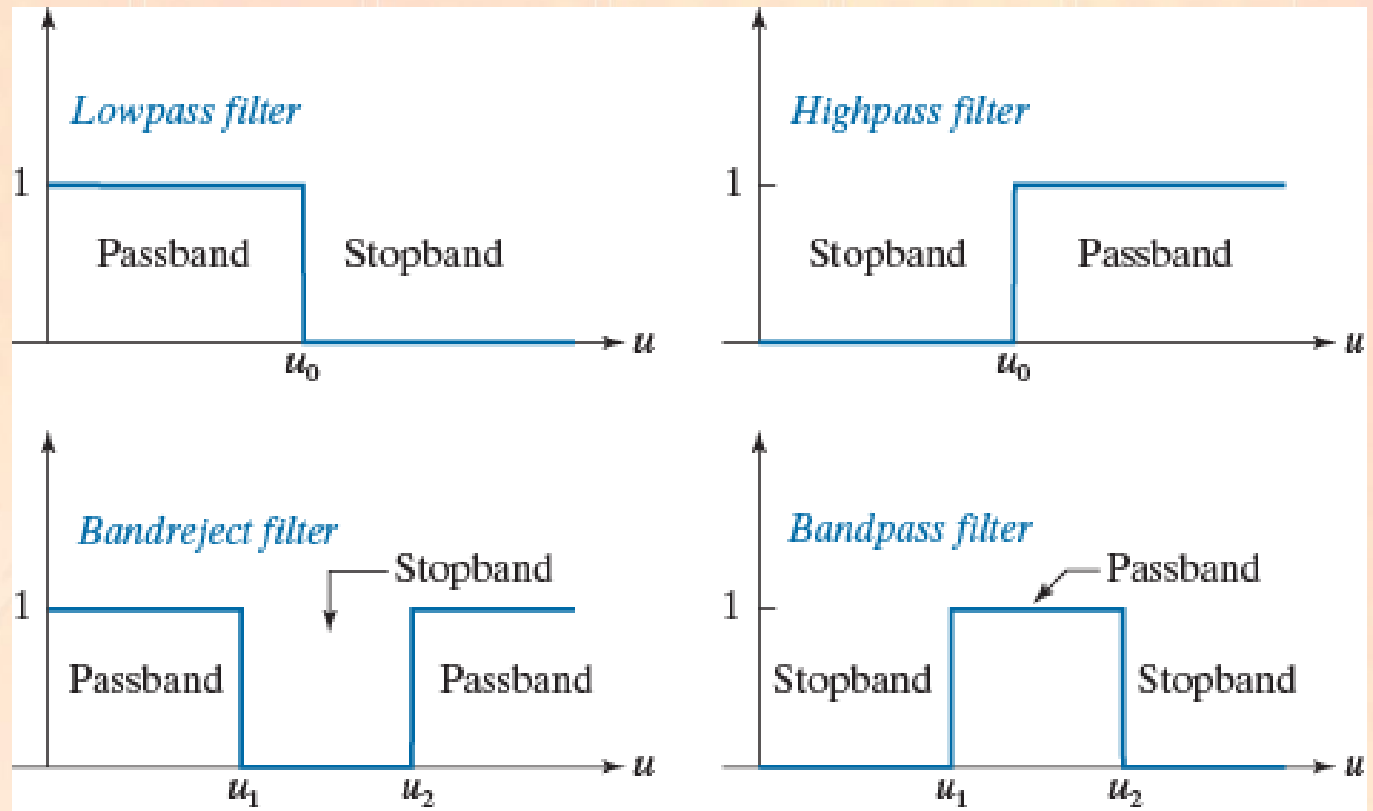
(a) Lowpass filter.

(b) Highpass filter.

(c) Bandreject filter.

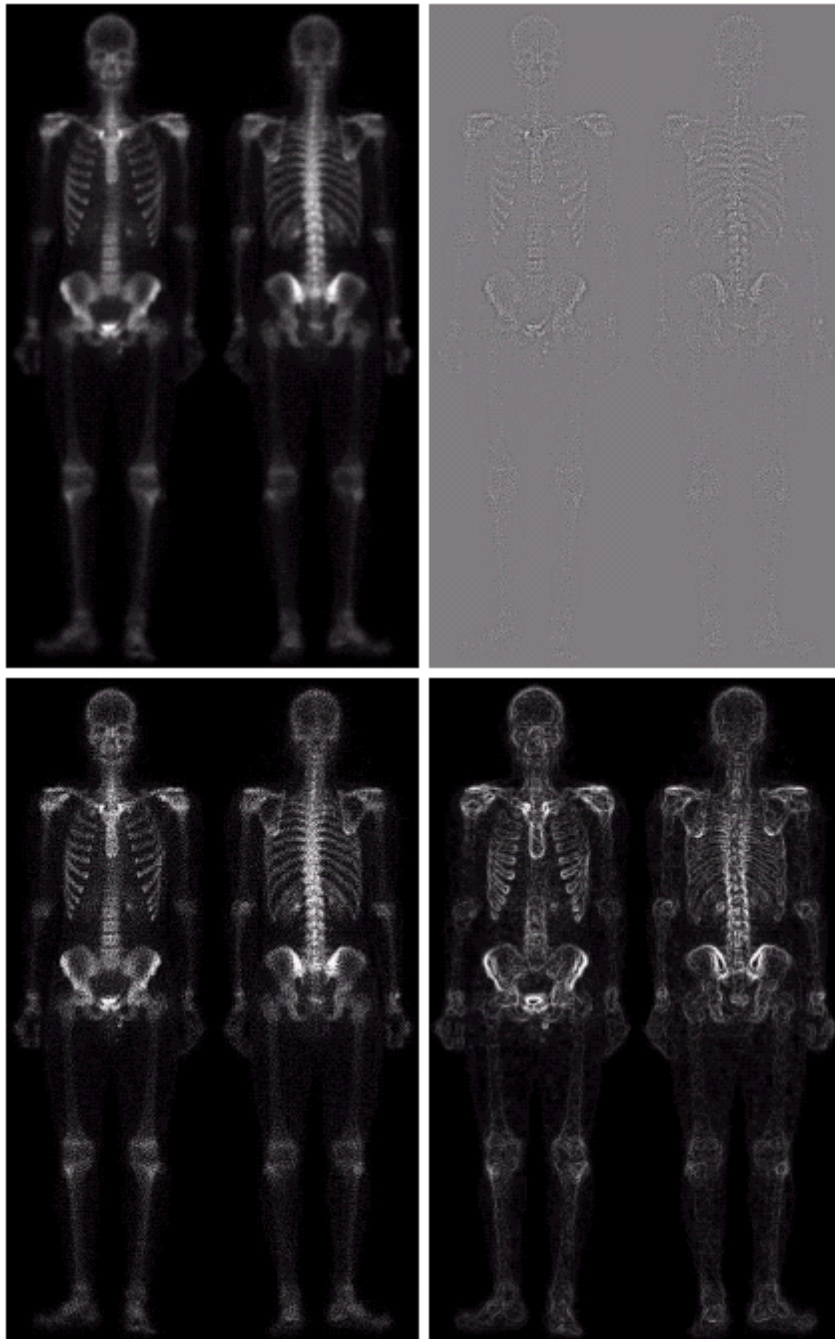
(d) Bandpass filter.

(As before, we show only positive frequencies for simplicity.)





- Frequently, a given enhancement task will require application of several complementary enhancement techniques in order to achieve an acceptable result.
- Examples:
  - nuclear whole body bone scan - [Fig. 3.46](#)

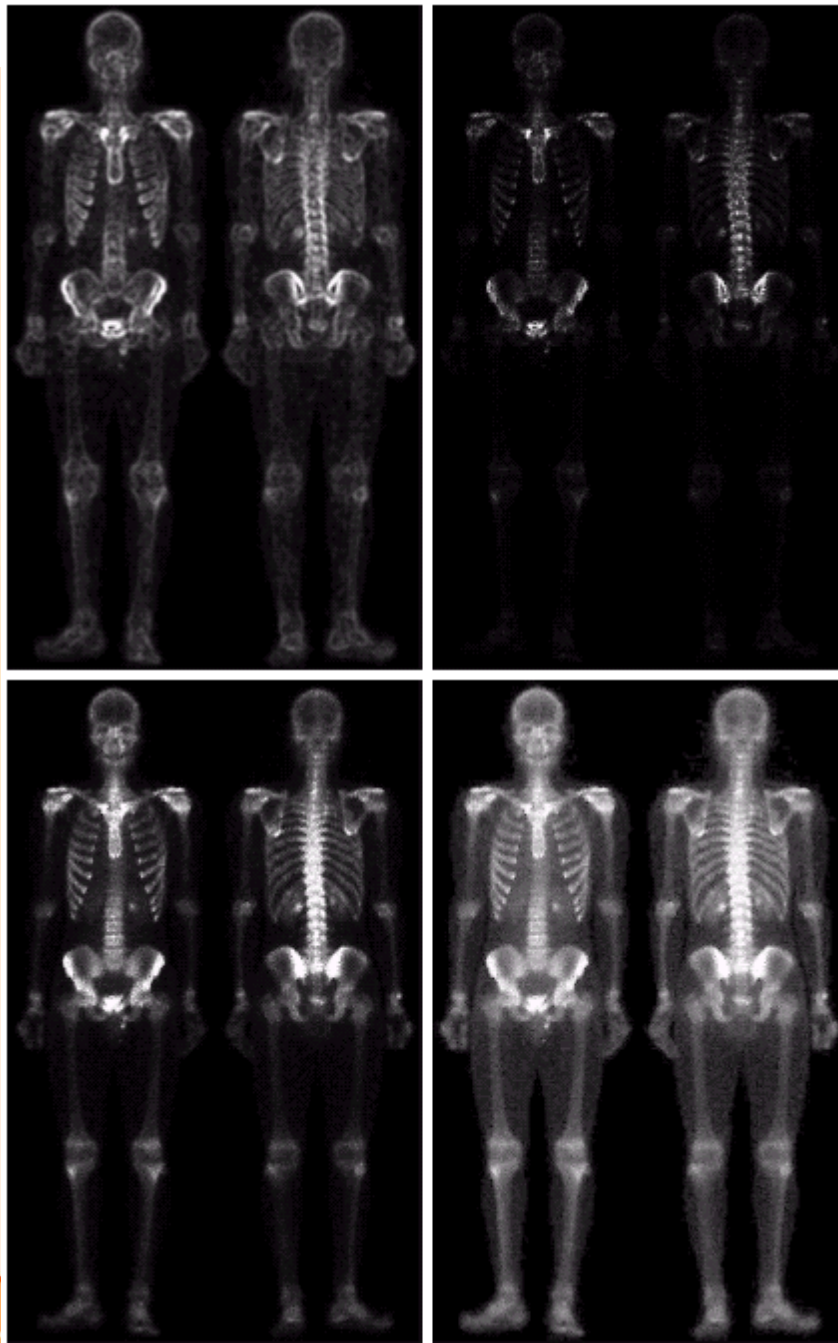


a	b
c	d

### FIGURE 3.46

(a) Image of whole body bone scan.

(b) Laplacian of (a). (c) Sharpened image obtained by adding (a) and (b). (d) Sobel of (a).



e f  
g h

### FIGURE 3.46

(Continued)

(e) Sobel image smoothed with a  $5 \times 5$  averaging filter. (f) Mask image formed by the product of (c) and (e).

(g) Sharpened image obtained by the sum of (a) and (f). (h) Final result obtained by applying a power-law transformation to (g). Compare (g) and (h) with (a). (Original image courtesy of G.E. Medical Systems.)